Corrosion Science 258 (2026) 113443

Contents lists available at ScienceDirect

Corrosion Science

journal homepage: www.elsevier.com/locate/corsci

Assessing the combined effect of gamma radiation and sulfate-reducing bacteria on copper corrosion for deep nuclear waste storage

Mar Morales-Hidalgo [a,*], Cristina Povedano-Priego [a], Marcos F. Martinez-Moreno [a,1], Adam D. Mumford [b], Kateřina Černá [c], Yon Ju-Nam [b], Jesus J. Ojeda [b], Ana María Fernández [d], Ursula Alonso [d], Fadwa Jroundi [a], Mohamed L. Merroun [a]

[a] Department of Microbiology, Faculty of Sciences, University of Granada, Granada, Spain
[b] Department of Chemical Engineering, Faculty of Science and Engineering, Swansea University, Swansea, United Kingdom
[c] Technical University of Liberec, Institute for Nanomaterials, Advanced Technologies and Innovations, Liberec, Czech Republic
[d] Departamento de Fisión Nuclear, CIEMAT, Avenida Complutense, 40, Madrid 28040, Spain

ARTICLE INFO

Keywords:
Geological disposal facility
Deep geological repository
Microbially influenced corrosion
Spectroscopic characterization
Microbial activity
Nuclear waste repository

ABSTRACT

Ensuring the integrity of containment barriers in geological disposal facilities (GDFs) is crucial for the long-term storage of radioactive waste. Copper is considered as a promising canister material due to its corrosion resistance. This study examines the combined effects of external gamma radiation (14 and 28 kGy) and sulfate-reducing bacteria (SRB) on copper corrosion in highly compacted FEBEX bentonite. Results showed that gamma radiation significantly reduces SRB viability, suggesting that these bacteria are likely to remain inactive during the early centuries of GDF operation, when radiation is at its highest level. Microscopic and spectroscopic analyses identified copper oxides, particularly CuO, as the main corrosion products. Gamma radiation was found to delay microbially influenced corrosion by altering the microbial community structure and promoting salt precipitation, including copper sulfates. SRB facilitated the formation of biogenic copper sulfides on unirradiated samples or those minimally affected by radiation. These findings provide valuable insights into the role of SRB in copper corrosion, broadening the understanding of long-term GDF safety.

1. Introduction

The long-term management of high-level radioactive waste remains one of the most critical global challenges due to the extended hazardous lifespan of spent nuclear fuel, which can exceed 100,000 years. Geological disposal facilities (GDFs), also known as deep geological repositories (DGR), are currently considered as the most reliable solution, offering multi-barrier containment systems to prevent radionuclide migration and ensure effective isolation from the biosphere. Among these engineered barriers, the metal canister plays a crucial role by enclosing the waste and being embedded in compacted bentonite clay within a stable geological formation [1,2]. The performance of this multibarrier system must remain stable under the evolving physico-chemical conditions expected throughout the repository lifetime, transitioning from early stages of high radiation, heat, and oxygen exposure, to late anoxic, cooler, and water-saturated conditions [3]. Understanding the corrosion behavior of the canister material under these evolving conditions is essential to assess the long-term performance and safety of the repository system. Copper has been selected as the canister material in several international licensed or under-construction GDF programs (e.g., the Finish (POSIVA) and Swedish (SKB) concepts) due to its high corrosion resistance [4,5]. The safety of the repository can be guaranteed when the involved corrosion processes are understood, and the relevance thresholds have been determined. While numerous studies have addressed its chemical and physical stability [6], less attention has been paid to biological factors, particularly microbial activity upon radiation in these deep environments. Sulfate-reducing bacteria (SRB) are of special interest due to their ability to induce microbially influenced corrosion (MIC) via sulfide production, potentially leading to the formation of copper sulfides on canister surfaces [7]. The key focus is on how SRB perform in a highly compacted bentonite environment under stressors typical of early repository phases, namely waste gamma radiation, and their effects on copper integrity. While some research has explored SRB survival under thermal and compaction conditions [8,9],

* Corresponding author.
[1] Current address: Helmholtz-Zentrum Dresden-Rossendorf e.V. (HZDR), Institute of Resource Ecology, Bautzner Landstrasse 400, Dresden 01328, Germany

https://doi.org/10.1016/j.corsci.2025.113443
Received 28 July 2025; Received in revised form 7 October 2025; Accepted 22 October 2025
Available online 24 October 2025

the coupled impact of radiation exposure on SRB communities remain insufficiently studied. Haynes et al. [10] reported survival of genera such as *Desulfosporosinus* and *Bacillus* after exposure to 1 kGy (24.17 Gy/min) radiation in bentonite, but the study did not address associated corrosion outcomes. Therefore, understanding microbial viability under higher radiation doses and their correlation with copper corrosion is critical for assessing long-term repository safety.

FEBEX bentonite has been established as the reference buffer engineered barrier material for deep geological storage in Spain. It is characterized by high smectite content (montmorillonite 80–90 wt%) and sourced from the El Cortijo de Archidona site [11]. In their previous work on FEBEX bentonite, Morales-Hidalgo et al. [12] examined the impact of the relevant GDF conditions on the total bentonite microbial communities, emphasizing the adverse effects of gamma radiation on bacterial diversity and viability. To replicate the conditions of a GDF during the early post-closure phase, FEBEX bentonite was compacted to a dry density of 1.6 g/cm^3, where a pure copper disk simulating the canister was placed in the center of the block. To simulate the radiation environment [13], the bentonite blocks were exposed to varying cumulative gamma radiation doses representative of first decades of repository operation after closure in the oxidizing period over different exposure times, followed by distinct incubation periods. Some treatments included a SRB bacterial consortium to enhance and accelerate microbial activity within the blocks and better appreciate their behavior. While previous studies have provided valuable insights into the strong associations between bentonite bacterial communities and environmental factors relevant to GDF conditions, several key questions remain unanswered. To the best of our knowledge, this is the first study to investigate the dynamics of copper corrosion under GDF-relevant coupled conditions, specifically bentonite compaction and gamma radiation. Building upon earlier findings, the present study aimed to further address these knowledge gaps by assessing how the same repository relevant conditions influence copper corrosion and exploring their potential link to MIC, particularly that caused by SRB. Given the critical role of copper canisters in ensuring the long-term safety of nuclear waste storage, understanding the influence of microbial activity, under these challenging repository conditions is essential.

While previous studies have investigated some of these factors separately, this work is the first to consider them jointly. For instance, Martinez-Moreno et al. [8,9] examined the effects of native microorganisms from FEBEX bentonite on copper corrosion under compacted conditions, however, the impact of gamma radiation was not considered. Bartak et al. [14] investigated the impact of gamma radiation at a dose rate of 0.4 Gy/h on BCV and MX-80 bentonites under anaerobic conditions. Nevertheless, due to the lack of compaction and the concurrent use of elevated temperature, the individual influence of radiation remained unclear, and no analysis of corrosion processes was carried out. Similarly, Bartak et al. [15] exposed BCV bentonite to cobalt-60 gamma radiation at 147 Gy/min, applying accumulated doses of 10, 30, 70, 100, and 140 kGy, but the study focused solely on the effect of radiation as a sterilization method and did not assess its effect on SRB or corrosion. The only previous work linking gamma radiation and the microbiology of FEBEX bentonite, conducted by Haynes et al. [10], was also performed under uncompacted conditions and did not include any analysis of corrosion. In light of these gaps, the present work introduces two major innovations in the investigation of GDF. To the best of our knowledge, this is the first work to combine gamma radiation exposure with compacted FEBEX bentonite at a dry density of 1.6 g/cm^3, a threshold value considered in several national repository concepts, while simultaneously assessing both microbiological and corrosion processes. The approach integrates both cultivability assays and DNA-based molecular analyses to investigate SRB – the main contributors to biotic corrosion – alongside advanced microscopic and spectroscopic characterization of copper surfaces.

By combining these critical factors into a unified experimental framework, the present study provides the first comprehensive evidence of the interactions between gamma radiation, microbiology, and corrosion under repository-relevant conditions. The multidisciplinary approach adopted in this work strengthens the scientific basis for understanding coupled and complex processes in GDFs, offering new insights relevant to the long-term safety of nuclear waste disposal.

2. Materials and methods

Experimental procedures related to the bentonite assembly and compaction have been previously described in detail in Morales-Hidalgo et al. [12]. A brief summary is provided below, while additional details regarding the methodology and analytical conditions are available in the Supplementary material.

2.1. Experimental setup

The study focuses on the Spanish bentonite FEBEX from the geological deposit of 'Cortijo de Archidona' in Almeria, Spain. Composed of 90 % montmorillonite, it belongs to the calcium-magnesium-sodium montmorillonite type, with trace amounts of other minerals [16,17]. The experimental batch used, referenced as FEBEX 70-IMA-3–4–0, was sieved to a grain size of < 0.5 mm.

The samples consisted of FEBEX Ca-Mg bentonite cylindrical blocks (38 $\times$ 25 mm in diameter and height) compacted to a dry density of 1.6 g/cm^3. Before compaction, bentonite powder was fully saturated with synthetic pore water (100 %), prepared following the composition detailed in Fernandez & Rivas [18], and inoculated either with a bacterial consortium (referred to as "B", described below) or its filtered culture medium, that is, the medium in which the bacteria had grown, subsequently passed through 0.22 μm pore-size filters to remove bacterial biomass. Sodium acetate (1.5 mM) was also supplemented to the bentonite powder as an electron donor source. Each bentonite block contained in its core a pure copper disk to evaluate corrosion. Oxygen-free pure copper (Cu) disks from Goodfellow Cambridge Ltd. Company (UNS number C10100; https://www.goodfellow.com) were used as representative of the future metal canisters. The elemental composition of each disk was 99.9 – 100 % Cu, with small impurities of S (< 0.0015 %), Pb (< 0.0005 %), Sb (< 0.0004 %), P (< 0.0003 %), and Zn (< 0.0001 %). Each Cu disk was designed with a diameter of 10 $\pm$ 0.5 mm and a thickness of 4 $\pm$ 10 % mm. The average weight was 2.8 g/disk. Prior to use, each disk was chemically cleaned to remove impurities and organic traces following the protocol outlined by Guo, M. [19].

Regarding the bentonite blocks inoculated with a bacterial consortium ("B"), they included five genera (*Desulfosporosinus acidiphilus* DSMZ 22704, *Desulfotomaculum reducens* DSMZ 100696, *Desulfuromonas* sp. DSMZ 101009, *Desulfovibrio desulfuricans* DSMZ 642, and the iron-reducing bacterium *Geobacter metallireducens* DSMZ 7210), previously identified in FEBEX bentonite [8,20,21], and purchased from the Leibniz Institute DSMZ collection (https://www.dsmz.de/). The strains were grown under anoxic conditions in their respective culture media (name between brackets) following the manufacturer's conditions. Each strain was added to the bentonite in its corresponding culture medium. The volumes added from each strain were as follows: 0.5 mL of *D. acidiphilus* [DSMZ 1250], 0.3 mL of *D. reducens* [DSMZ 63], 0.3 mL of *Desulfuromonas* sp. [DSMZ 1041], 0.5 mL of D. *desulfuricans* [DSMZ 63] and 0.2 mL of *G. metallireducens* [DSMZ 579]. As mentioned above, to avoid decompensation of the compounds available in the bentonite blocks, the same volumes of culture medium, but filtered through sterile 0.22 μm nitrocellulose filters, were added to the non-consortium treatments.

It was calculated that a final volume of 5 mL was required to achieve 100 % saturation. This final volume included 3.2 mL of artificial pore water, a total of 1.8 mL of the different bacterial consortium strains in their culture media (filtered or not) and 150 μl of sodium acetate (1.5 mM). Reference pore water and the bacterial consortium were prepared separately and stored in a laminar flow cabinet. A 3.2 mL

aliquot of pore water and 150 μL of sodium acetate (1.5 mM) were added to 51.28 g powdered FEBEX bentonite. At this step, if required, the bacterial consortium (1.8 mL) was inoculated. Non-consortium samples were traced with 1.8 mL of filtered culture media. The moistened clay was gently mixed under sterilized conditions with a spatula until the sample was homogenized.

The required bentonite powder for each block was measured in a porcelain crucible, along with a cleaned Cu coupon. The volume of the Cu disk (0.31 cm^3) was subtracted from the clay mass calculations to ensure the desired dry density. Each sample had an average clay mass of 51.28 ± 0.001 g at a density of 1.6 g/cm^3, with the 5 mL of volume required for full saturation. The compaction procedure consisted of pouring 25.64 g of the wet bentonite mixture into an aseptic stainless-steel mold, placing the copper disk in the center, and subsequently adding another 25.64 g of wet bentonite on the top. Finally, the blocks were compacted to the desired density of 1.6 g/cm^3 using a press. Each block was then placed in a polyethylene vessel filled with N_2, sealed with parafilm and afterwards stored in an anaerobic jar with anaerobiosis generator sachets (AnaeroGen™, Thermo Scientific) to ensure anoxic conditions throughout the incubation period. All the blocks were incubated at 30 °C and kept in the dark. All equipment was sterilized with analytical grade ethanol (70 %) throughout the process. The bentonite block assembly and compaction were carried out at the Physicochemistry of Actinides and Fission Products Unit (CIEMAT, Madrid, Spain). As a starting point, non-incubated natural bentonite powder was analyzed under two conditions: non-irradiated (T.0N) and after gamma irradiation with 14 kGy (T.0IR) (Fig. 1).

Various irradiation treatments were applied to the samples, classified according to the number of irradiation cycles and cumulative dose: R (single cycle of 14 kGy) and 2R (two cycles of 14 kGy, resulting in a cumulative dose of 28 kGy) (Fig. 1). Single-irradiated samples (R) were further subdivided based on the timing of irradiation: early radiation (e_R) applied prior to incubation, and late radiation (l_R) applied after 6 months of anoxic incubation. In the case of double-irradiated treatments (2R), the first cycle was applied before incubation, with the second cycle following 6 months of incubation, after which the samples were further incubated for an additional 6 months. Irradiation was carried out at the CIEMAT Nayade ^{60}Co gamma irradiation facility (https://rdgroups.ciemat.es/en/web/materiales/radioactive-laboratory), where samples were irradiated for 8 days and 19 h at a dose rate of 66 Gy/h, resulting in a total accumulated dose of 14 kGy. The irradiation was conducted in a cylindrical chamber specifically designed to provide uniform exposure of the samples to the radiation field. Twelve cylindrical cobalt-60 (^{60}Co) sources, each 15 mm in diameter and 135 mm in length, are arranged

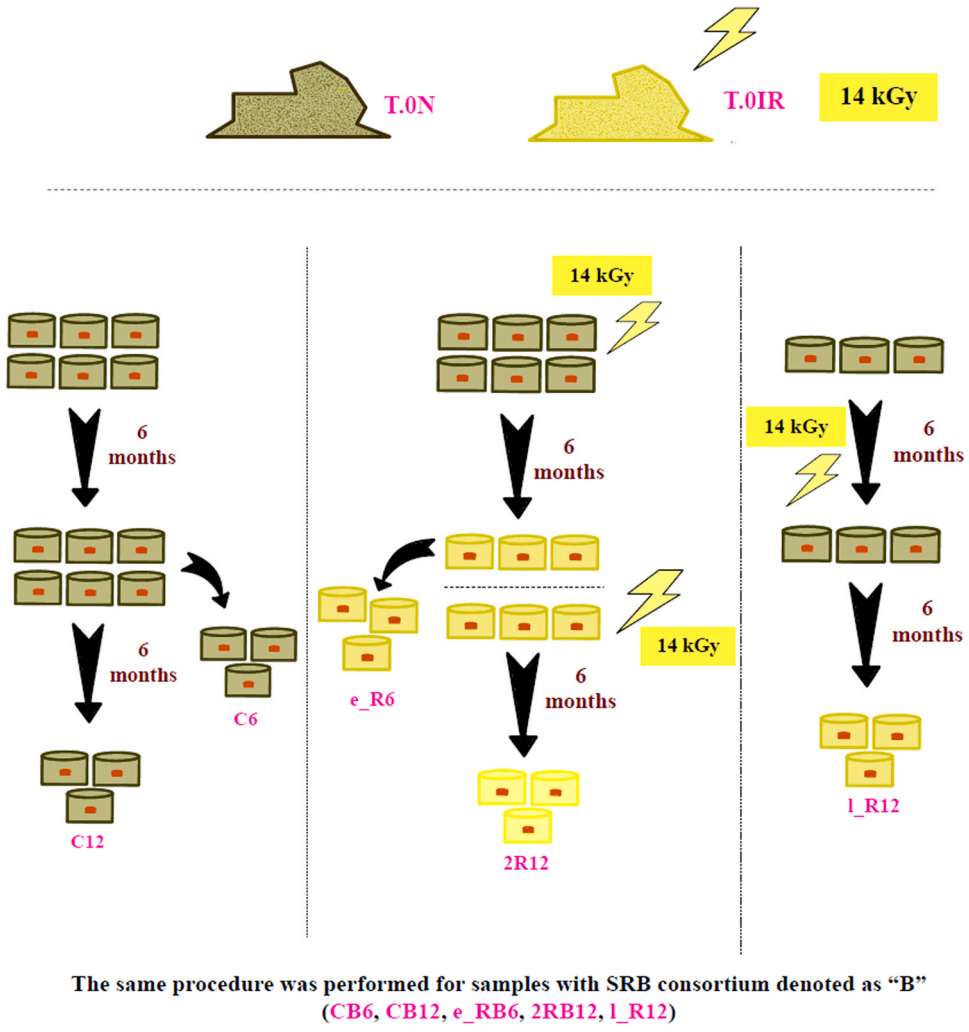

Fig. 1. Schematic representation of the experimental set-up of the different FEBEX bentonite treatments. The same procedure was repeated with SRB consortium inoculation (denoted as "B"). Figure modified from Morales-Hidalgo et al. [12]. T.0N: non-incubated nor irradiated powdered bentonite; T.0IR: non-incubated irradiated powdered bentonite (14 kGy); C: non-irradiated compacted controls; B: SRB consortium; e_R: treatments irradiated once before the start of incubation, as early exposure (14 kGy); l_R: treatments irradiated once in the middle of the incubation time as late exposure (14 kGy); 2R: two-times irradiated treatments (28 kGy); 6: six months of anoxic incubation; 12: one year of anoxic incubation.

around the outer part of the chamber in a circular configuration. This arrangement creates an inner cylindrical irradiation volume where the samples are placed. Dosimetry was carried out, before irradiation, using eight Fricke chemical dosimeters, positioned at representative locations, in order to determine the absorbed dose and verify the uniformity of irradiation within the cylindrical chamber. The requested dose rate was applied according to the necessary experimental conditions. Absorbance readings were obtained using the standard molar extinction coefficient of 2181 $L{\cdot}mol^{-1}{\cdot}cm^{-1}$, and the absorbed dose was calculated following the established Fricke dosimetry procedure. This setup ensured accurate dose determination and allowed assessment of the dose distribution within the irradiated region. The standard deviation of dose measurements provided by 8 different dosimeters, located at different positions within the chamber, was lower than 3 %. According to this, radiation cylindrical configuration ensures homogeneous dose distribution within the whole irradiated volume inside the chamber, and therefore within all irradiated samples.

Additionally, non-irradiated controls (referred to as "C") were treated in the same manner but without irradiation. All treatments were prepared in triplicates, except for the double-irradiated treatments (2R12 and 2RB12), which were prepared in duplicates due to technical limitations. The incubation of all samples was performed at 30 °C under anoxic conditions. Further sample details and experimental conditions are provided in Supplementary Table S1.

2.2. Microbiological studies

The bentonite blocks were stored at −20 °C for molecular analyses and at 4 °C for culture-dependent viability studies. Prior to each analysis, the blocks were ground into a powder ensuring a uniform consistency by using a porcelain mortar sterilized with ethanol (70 %).

2.2.1. Molecular microbial analyses: DNA extraction and quantitative PCR

To quantify the presence of SRB in the different treatments using qPCR, total DNA was extracted from each bentonite block sample. The standard phenol-chloroform extraction protocol [22] was followed, incorporating the optimization steps for compacted bentonite samples as detailed in reference [12]. Subsequently, quantitative polymerase chain reaction (qPCR) targeting adenosine 5′-phosphosulfate reductase gene (*apsA)* and the dissimilatory sulfate reductase gene (*dsrA)* markers, was employed to assess the changes in SRB abundance across different treatments and incubation periods. All reactions were performed using a LightCycler 480 instrument (Roche, Switzerland). The quantification of relative gene copy numbers was based on the calculation of relative abundance of non-template controls (NTCs), which only amplified background signal, using the ΔCq calculation method as described in Shrestha et al. [23]. Each sample was run in duplicate, ensuring the difference between Cq values was less than 0.5. Due to the complexity of environmental samples, as explained in [23], absolute quantification without a standardized calibration curve would yield unreliable results. Therefore, relative quantification (RQ) was used to determine the relative abundance of SRB genes. The delta Cq method was employed to calculate RQ, which is the magnitude of the difference in Cq values between samples, using the formula RQ = efficiency (−ΔCq) [24,25]. This method accounts for primer amplification efficiency, determined from standard curves generated by serial dilutions of template DNA from five internal environmental standards. qPCR conditions and data analysis were conducted according to the methodology previously described [12], with more details available in **section 1.1** of the Supplementary material.

2.2.2. Microbial viability analysis: most probable number of sulfate-reducing bacteria

The abundance of cultivable SRB was estimated using the Most Probable Number (MPN) method (Biotechnology Solutions, Houston, USA). Bentonite samples from each treatment (mixed from three biological replicates) were processed under anoxic conditions in a nitrogen-filled glove box. A 0.5 g of treated bentonite was suspended in sterile N_2-degassed PBS, and serial dilutions (10^{-1} to 10^{-5}) were prepared in triplicate using Postgate's medium (DSMZ Medium 63, www.dsmz.de/). Cultures were incubated for 30 days at 30 °C in dark, under static conditions. After incubation, the appearance of black precipitates indicated the presence of FeS resulting from active sulfate reduction. MPN values were determined according to standard reference tables. DNA from selected positive cultures was extracted using Qiagen DNeasy PowerSoil Pro Kit and sequenced targeting the 16S rRNA gene to evaluate SRB diversity. Further methodological details and bioinformatic procedures are available in **section 1.2** of the Supplementary material.

2.3. Copper disks corrosion studies

The surfaces and corrosion products of Cu disks disassembled from the compacted bentonite blocks subjected to the above-mentioned treatments were analyzed using variable pressure field emission scanning electron microscopy (VP-FESEM) and X-ray photoelectron spectroscopy (XPS), following previously described procedures [8]. Briefly, disks were fixed in a 2.5 % glutaraldehyde solution prepared in 0.1 M cacodylate buffer (pH 7.4) for 24 h at 4 °C. The disks were then dehydrated using an increasing ethanol gradient (30 to 100 %), followed by drying using the critical point drying (CPD) method [26] with CO_2 in a Leica EM CPD300. Finally, the dried samples were coated with carbon by evaporation using an EMITECH K975X Carbon Evaporator.

XPS analyses were performed on non-fixed Cu disks, following the procedure of Martinez-Moreno et al. [8]. The XPS system used was a Kratos AXIS Supra Photoelectron Spectrometer equipped with a monochromatic Al Kα X-ray source (1486.6 eV), with an X-ray emission current set to 20 mA and the anode high tension at 15 kV. The take-off angle was fixed at 90° with respect to the sample plane, and data were collected from three randomly selected points on each sample. Each area analyzed had an approximate size of 110 μm × 110 μm (FOV2 lens). Both broad survey scans (step energy of 160 eV, step size of 1.0 eV) and high-resolution scans (step energy of 20 eV, step size of 0.1 eV) were conducted for chemical state analysis. A Kratos integral charge neutralizer was employed to prevent surface charging. Calibration of the binding energy scale was performed using the Au $4f_{5/2}$ (83.9 eV), Cu $2p_{3/2}$ (932.7 eV), and Ag $3d_{5/2}$ (368.27 eV) lines from standard gold, copper, and silver samples provided by the National Physical Laboratory (NPL), UK. XPS spectra were processed and analyzed using CasaXPS version 2.3.22 software [27]. Binding energies were referenced to the C1 s adventitious carbon peak at 284.8 eV to correct for surface charging effect.

3. Results and discussion

This study examined the effects of bentonite compaction and gamma radiation on SRB viability and copper corrosion. FEBEX bentonite was first fully saturated with pore water and subsequently compacted to a dry density of 1.6 g/cm^3. To evaluate the stability of the compaction over time, the dimensions of the blocks were recorded after 6 and 12 months of incubation. The measurements confirmed that all samples remained at their original size (38 × 25 mm), thereby maintaining a constant dry density of 1.6 g/cm^3 throughout the duration of the experiment. Additionally, no cracks or signs of high amount of gas production were observed that could compromise the stability of the compacted density.

3.1. Changes in sulfate-reducing bacteria abundance over time by qPCR

The relative SRB abundance compared to non-template controls (NTCs) was determined by quantifying two key genes involved in sulfate reduction from the total extracted DNA, adenosine 5′-phosphosulfate reductase gene (*apsA*) and the dissimilatory sulfate reductase gene

(*dsrA*). This analysis allowed the assessment of changes in abundance of this bacterial group across treatments and over the incubation period. Based on this approach, the qPCR analyses were performed on the samples, at time 0 and after 6 months and 1 year of incubation (Fig. 2).

The abundance of autochthonous SRB in raw FEBEX bentonite was very low, as confirmed in non-treated, non-incubated powdered bentonite (T.0N), where the signal for both genes was undetectable. However, the presence of native bentonite SRB was confirmed by detectable gene signals in treatments involving non-irradiated compacted blocks without the consortium but incubated for 6 months (C6) and 1 year (C12). The bentonite used in this study had been stored for years without water or nutrients, resulting in an undetectable abundance of this bacterial group in non-treated non-irradiated time 0 (T.0N). However, in samples fully saturated with pore water, amended with sodium acetate, and incubated for 6 months or 1 year, a detectable signal for both genes was observed, albeit at low relative abundance (Fig. 2). This increase in abundance indicated that bacterial activity occurred during these incubation periods, leading to cell proliferation, as reflected in the increased number of gene copies.

Exposure to a total radiation dose of 14 kGy, whether applied early (T.0IR, e_R6) or late (l_R12), was sufficient to render the signal for both genes, *apsA* and *dsrA*, undetectable in non-consortium treatments. Similarly, no gen signal was observed following a double dose of irradiation (2R12). This suggests that radiation may have suppressed the proliferation of indigenous SRB throughout the incubation period. Nevertheless, both genes were detectable to varying degrees in all consortium-inoculated treatments (B), including the irradiated ones, where the SRB load was higher (CB6, e_RB6, CB12, l_RB12, 2RB12). Despite this, the consortium treatments followed a consistent trend reflecting the negative impact of gamma radiation on SRB. As shown in Fig. 2, the relative quantification of SRB genes was lower in the irradiated samples e_RB6 and 2RB12 compared to their non-irradiated counterparts CB6 and CB12. An exception was observed in sample l_RB12, which exhibited gene abundance levels comparable to those of the non-irradiated control CB12, in agreement with the patterns of this treatment observed across the other analyses. The presence of such DNA in the qPCR analysis and the quantification of the genes under study did not imply the survival of these genera. In any case, it provides a useful reference for understanding shifts in the bacterial communities, as an increase in the number of gene copies is likely indicative of bacterial cell proliferation.

To date, limited information is available on the quantification of SRB genes in bentonite samples, and to our knowledge, this is the first study to report such findings specifically in compacted FEBEX bentonite. An interesting study performed by Shrestha et al. [23] quantified the *dsr* gene in bentonite suspensions with and without concrete and concluded that the presence of concrete inhibited SRB growth. This outcome was somewhat unexpected, considering that the concrete environment was rich in sulfate, which would typically support SRB activity. However, the elevated pH in the concrete-containing samples likely caused the observed inhibition. Most bentonite-related studies involving SRB analyses rely on culture-dependent methods [8,10,20,28,29] or 16S rRNA gene quantification [14], as also reported for these samples in the previous study by Morales-Hidalgo et al. [12]. Our data demonstrates the importance of incorporating gene-targeted molecular approaches to progressively build a more comprehensive understanding of the behavior of this key microbial group. Given the significant role of SRB in long-term anaerobic corrosion of copper containers [30], it is crucial to further investigate their behavior under different scenarios, even considering their low abundance in the samples and limited viability under harsh conditions such as those expected in future GDFs (e.g. radiation, bentonite compaction). To address this, the analysis of this bacterial group was complemented with cell viability assessments to determine whether viable SRB cells capable of thriving under favorable conditions persist after each treatment.

3.2. Estimation of SRB viability and survival: quantification by most probable number method

The presence of viable SRB cells was estimated after the different treatments and at different incubation times, using quantification by the most probable number (MPN) per gram of bentonite in Postgate medium (Table 1). No black precipitates were observed throughout the study in the negative control, corresponding to Postgate medium without inoculated bentonite, confirming the sterility of culture sample preparation. Positive SRB MPN evidence was found in unincubated, untreated natural bentonite (T.0N) as well as in the non-spiked and compacted treatments (C6 and C12), as indicated by the formation of black precipitates. This

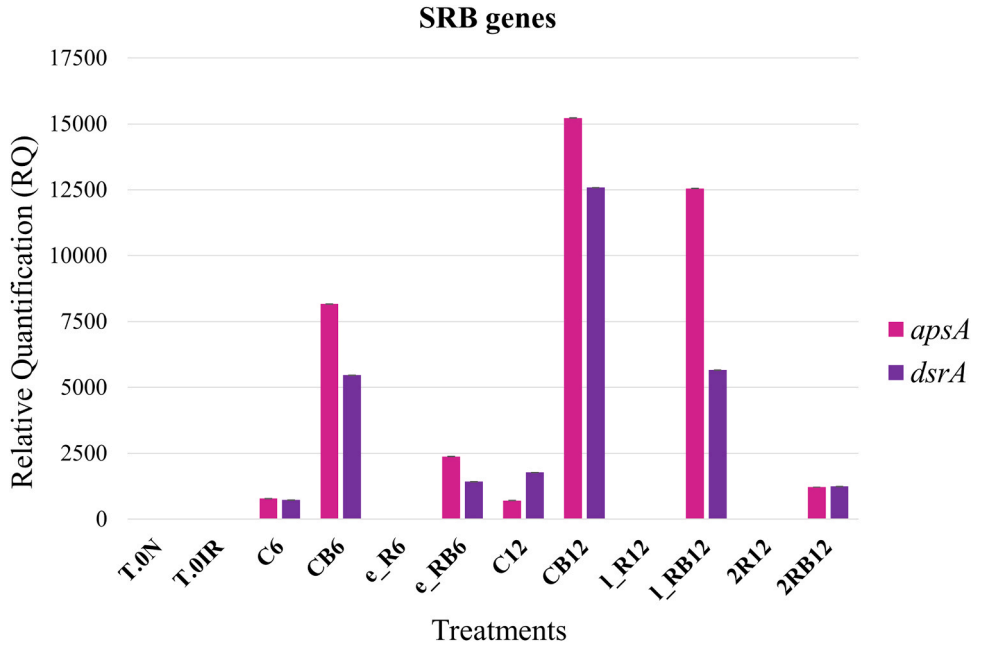

Fig. 2. Relative quantification of sulfate-reducing bacteria (detected by *apsA* and *dsrA*) in 1.6 g/cm^3 bentonite blocks in triplicate (except 2R12 and 2RB12 in duplicate) at time 0 (non-incubated) and after six months and one year of anoxic incubation.

Table 1
Most probable number (MPN) of SRB per gram of dry bentonite (MPN/g) in Postgate medium. All the values were calculated considering the initial suspension for cell's dispersion (1 g of bentonite in 9 mL of PBS). XYZ pattern: number of positive bottles after 3PB dilution; MPN value: MPN data from the reference table; 3PB dilution: dilution with 3 positive bottles prior to XYZ pattern.

Sample	XYZ pattern	MPN value	3PB dilution	MPN g/bentonite
T.0N	321	15	10^{-1}	1.50×10^{4}
T.0IR	000	< 3	-	< 3
C6	333	$+ 140$	10^{-2}	$> 1.40 \times 10^{5}$
CB6	333	$+ 140$	10^{-2}	$> 1.40 \times 10^{5}$
e_R6	000	< 3	-	< 3
e_RB6	320	9.5	10^{0}	9.50×10^{1}
C12	300	2.5	10^{0}	2.25×10^{1}
CB12	320	9.5	10^{0}	8.55×10^{1}
l_R12	000	< 3	-	< 0.3
l_RB12	000	< 3	-	< 0.3
2R12	000	< 3	-	< 0.3
2RB12	100	0.4	10^{0}	0.4

finding confirmed the presence of native, viable SRB cells in the FEBEX bentonite. As previously mentioned, neither of the two sulfate-reducing genes (*apsA* nor *dsrA*) was detected in the T.0N sample, initially suggesting the absence of this group. However, cultivation under more favorable conditions, including the use of a selective medium, the initially low abundance of SRB appeared to proliferate, indicating their viability and enabling detection. Furthermore, the positive culture results in the C6 and C12 treatments confirmed that SRB cells can survive compaction conditions over extended periods of up to one year. Nevertheless, the values after 1 year of incubation C12 (2.25×10^{1} MPN/g bentonite) were lower than those at T.0N and C6 (1.5×10^{4} and $> 1.4 \times 10^{5}$ MPN/g bentonite, respectively). As previously mentioned, the decrease in cell viability cannot be attributed to a single factor, as multiple variables, such as nutrient availability, water content and compaction, may have affected their persistence. At time 0, the natural bentonite had no added nutrients and, as naturally dry material, containing only minimal water availability (14 % humidity at atmospheric laboratory conditions); however, non-compacting conditions were tested. After 6 months, nutrient and water levels were presumed to be higher than at 1 year, due to the initial addition of 1.5 mM sodium acetate and the full saturation of the blocks with pore water at the start of the incubation. After 1 year, these resources were likely significantly depleted. Hence, by comparing SRB viability under conditions of water and nutrient limitation combined with compaction (C12) to that in untreated, non-compacted bentonite at time 0 (T.0N), it was suggested that this combination of compaction and resource limitation severely affected SRB survival. Similar results about the presence and viability of this bacterial group in the same bentonite type were discussed in previous studies [8,9]. Specifically, Martinez-Moreno et al. [8] reported on the viability of SRB after one year of incubation in anoxic conditions at bentonite density 1.7 g/cm^3. Consistent with our data, they observed a decrease in the SRB viability, measured by MPN/g bentonite, under compaction conditions after one year of incubation compared to the initial bentonite. Moreover, they reported a slight increase in SRB viability in bentonite blocks amended with a combination of electron donors.

Interestingly, no evidence of SRB growth was detected in the irradiated samples at time 0 (T.0IR, 14 kGy), 6 months (e_R6, early 14 kGy), nor 1 year (l_R12, l_RB12, late 14 kGy; or 2R12). Only a few bottles tested positive in the early irradiated, SRB-spiked treatment at 6 months (e_RB6), and just one in the double-irradiated, SRB-spiked treatment at 12 months (2RB12), suggesting that these isolated cases were not representative of SRB viability under such conditions. Therefore, these data imply a negative effect of gamma radiation exposure, at cumulative doses of 14 kGy or 28 kGy (radiation rate of 66 Gy/h), on the viability of this bacterial group, which can play a crucial inhibiting role in the biotic corrosion of copper.

To further identify the main viable SRB genera, 16S rRNA gene next-generation sequencing was performed on the positive bottles from MPN experiment from each treatment (Fig. 3). It is important to note that Postgate medium can also support the growth of microorganisms other than SRB, as some may utilize alternative substrates such as yeast extract and lactate. However, only bacteria capable of reducing sulfate to sulfide produce the characteristic black precipitate, indicating a positive bottle culture. The relative abundances of viable genera are shown in Fig. 3**,** and Supplementary Table S2. Only the viable SRB genera present in each of the positive treatments are represented in Supplementary Figure S1. The results revealed that the predominant SRB genera across all samples were *Desulfosporosinus* (10.53 %), *Desulfotomaculum* (8.67 %) and *Desulfofarcimen* (7.98 %). Other SRB genera were present in lower relative abundance, such as *Desulfallas-sporotomaculum* (0.61 %), *Desulfohalotomaculum* (0.53 %), and *Desulfurispora* (0.02 %). All of these genera are native to the FEBEX bentonite, as they have also been identified in samples that were not inoculated with the consortium. Only two of the five strains included in the bacterial consortium were identified as viable: *Desulfosporosinus* and *Desulfotomaculum*. The remaining three, *Desulfuromonas*, *Desulfovibrio*, and *Geobacter*, may have failed to adapt to the initial post-inoculation conditions or may not have survived the experimental parameters.

Desulfosporosinus emerged as the most abundant viable SRB genus. This is a well-known genus forming part of the native FEBEX bentonite microbial community [8,20,31]. In this study, both its native presence and viability are confirmed, as it was identified in the natural, non-treated, non-incubated bentonite sample (T.0N, 44.61 %), as well as in the compacted samples without the consortium, incubated for 6 months (C6, 5.51 %) and 1 year (C12, 0.57 %) (Fig. 3**,** Supplementary Table S2). However, in the treatments inoculated with the consortium (CB6, CB12, and e_RB6), it is not possible to determine whether the *Desulfosporosinus* genus detected corresponds to the inoculated strain, the indigenous population, or a combination of both. Nevertheless, this distinction is not of critical importance, as the key factor is the response of this SRB genus to experimental conditions, regardless of its origin. Notably, the presence of this bacterium in the treatment irradiated early with 14 kGy and incubated for 6 months (e_RB6, 21 %) indicated a potential intrinsic resistance to radiation, as its viability was maintained despite the exposure. In fact, *Desulfosporosinus* has also demonstrated remarkable versatility in surviving harsh conditions, as it remained viable after a long-term incubation of three years in FEBEX bentonite microcosms in the presence of uranium [20]. Moreover, these findings align with those previously reported by Haynes et al. [10], who investigated the impact of a total gamma radiation dose of 1 kGy (24.17 Gy/min) on the microbiota of different bentonite types, including FEBEX. They demonstrated that after FEBEX bentonite radiation exposure, only *Desulfosporosinus*, *Bacillus*, and *Clostridium* were detected in Postgate medium. Similarly, in the present study, *Bacillus* (79 %) was the other most abundant genus, as shown in Fig. 3.

The second most abundant viable SRB genus was *Desulfotomaculum*, which is also known to be native to FEBEX bentonite [8,20]. It was particularly prominent in the compacted treatments without the consortium, with a relative abundance of 25.45 % in C6 and 29.42 % in C12 (Supplementary Table S2). However, this genus was not detected in any of the positive irradiated treatments, not even in those with the added consortium, suggesting a higher sensitivity to gamma radiation. The FEBEX bentonite-indigenous SRB genera *Desulfofarcimen, Desulfohalotomaculum,* and *Desulfallas-sporotomaculum*, formerly belonging to the genus *Desulfotomaculum*, were reclassified by Watanabe et al. [32] as novel genera. Therefore, despite being identified separately, they share very similar characteristics, remaining both *Desulfofarcimen* and *Desulfallas-sporotomaculum* viable in the doubly irradiated treatment (2RB12). However, the quantification of SRB by MPN (Table 1) indicated a very low cell load. Consequently, it is uncertain to conclude that these genera are truly resistant to gamma radiation, as their presence

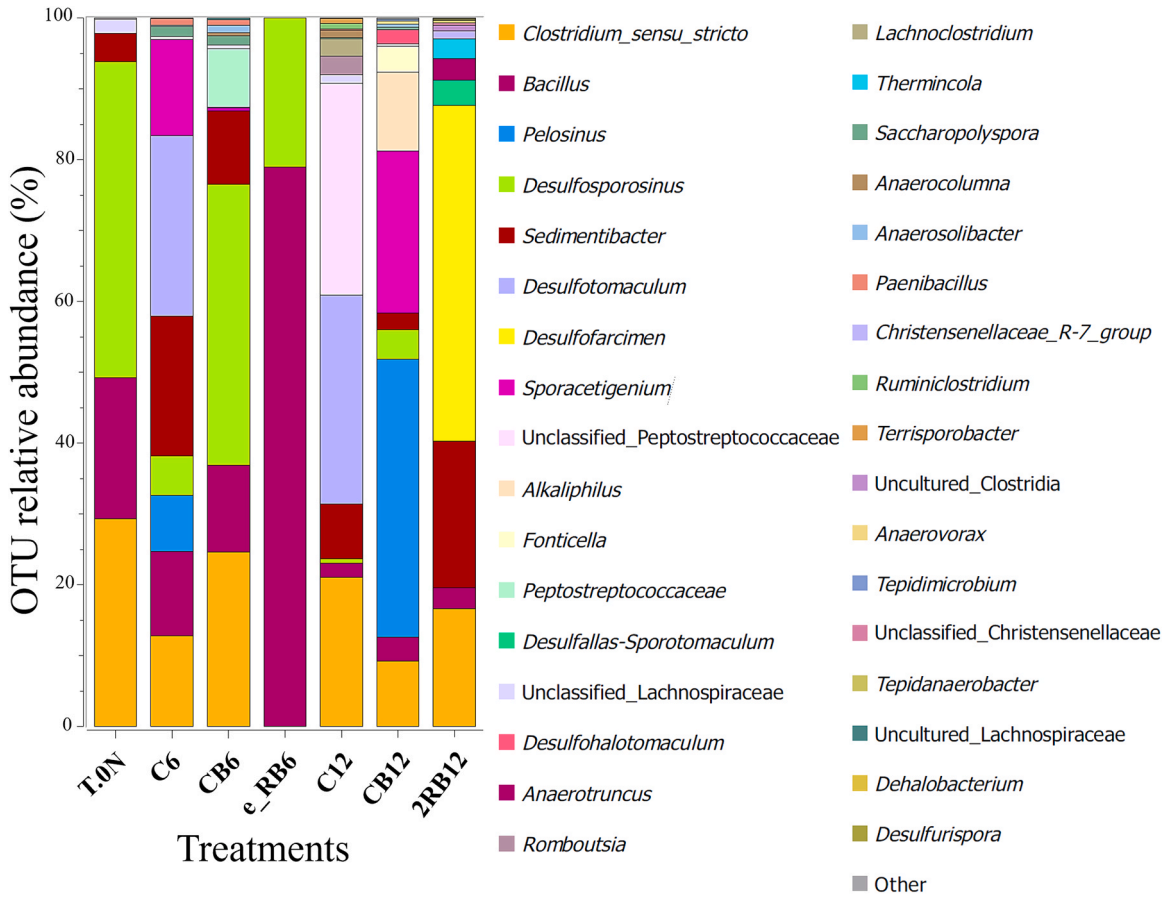

Fig. 3. OTU relative abundance at genus level for viable genera enriched in Postgate medium from positive treatments in MPN experiment. The selected cut off is $\geq$ 0.02 %.

could instead result from a small number of resistant cells that managed to proliferate under favorable conditions. Nevertheless, further research on these genera would be valuable to gain a deeper understanding of their behavior in response to gamma radiation.

Although *Clostridium* is not traditionally classified as a SRB, it was among the most abundant genera identified in positive SRB cultures (Fig. 3). Notably, existing literature reports that certain species within this genus possess the ability to reduce sulfate to sulfide [33]. Additionally, *Clostridium* can ferment lactate, present in the Postgate medium, producing acetate as a metabolic byproduct [34].

In conclusion, assessing the viability and identifying the native SRB genera in bentonite is essential for understanding their potential behavior under various conditions in a GDF. Since this group of bacteria is the main contributor to copper corrosion, this knowledge is essential for predicting and mitigating long-term risks on the integrity of nuclear waste storage systems.

3.3. Copper surface characterization along the incubation time

In the present study, the copper disks from the different treatments were analyzed both macroscopically by visual inspection and microscopically by variable pressure field emission scanning electron microscopy (VP-FESEM) and energy dispersive X-ray (EDX) microanalysis after 6 months and 1 year of incubation (Figs. 4 and 5). In general, the disks that exhibited a more damaged appearance upon visual inspection had not undergone irradiation, as shown in Supplementary Figure S2 (C6, CB6, C12, CB12).

The ESEM and EDX analyses of samples incubated for both 6 months and 1 year revealed consistent trends across treatments. The only difference was the higher amount of corrosion products observed in the 1-year treatments. The surface of each Cu disk was scanned by ESEM, resulting in a montage that integrated images from the entire disk surface to identify the principal corrosion products and their distribution. (Supplementary Figure S3). A variety of precipitates composed of Cu-O of differing morphologies were detected on all samples at both six-month and one-year incubation times (Figs. 4 and 5). These likely copper oxides (Cu_xO) were particularly prevalent in the non-irradiated samples, which exhibited more pronounced surface damage both with (CB6, CB12) and without SRB consortium (C6, C12). Consistent with the lack of differences observed in the microbiological analyses previously reported by Morales-Hidalgo et al. [12], the copper disks from the late irradiated treatments after 6 months of incubation (l_R12, l_RB12) showed corrosion features comparable to those of the non-irradiated 1-year treatments (C12, CB12).

One of the principal biocorrosion products of concern in relation to microbially influenced copper corrosion is copper sulfide [30]. For this reason, the sulfur (S) signal was investigated in these Cu disks to identify Cu-S compounds. Nevertheless, microscopy and EDX techniques do not allow for an accurate differentiation between copper sulfide and copper sulfate salt. S signal was detected in all treatments with SRB consortium, both at 6 months and 1 year of incubation (CB6, CB12, e_RB6, l_RB12, 2RB12). In addition to these inoculated samples, it was also detected in all irradiated treatments, regardless of incubation time and total radiation dose received (e_R6, e_RB6, l_R12, l_RB12, 2R12, 2RB12). Upon closer examination of the zones on each disk exhibiting sulfur signals, the following observations were made: in the non-irradiated treatments (CB6, CB12) together with early irradiated (e_RB6) and late-irradiated treatments (l_RB12), all containing the SRB consortium, small Cu-S precipitates were observed, located exclusively within bentonite layers (Figs. 4**B**, 4**D**, 5**B**). However, in the treatment with double doses of

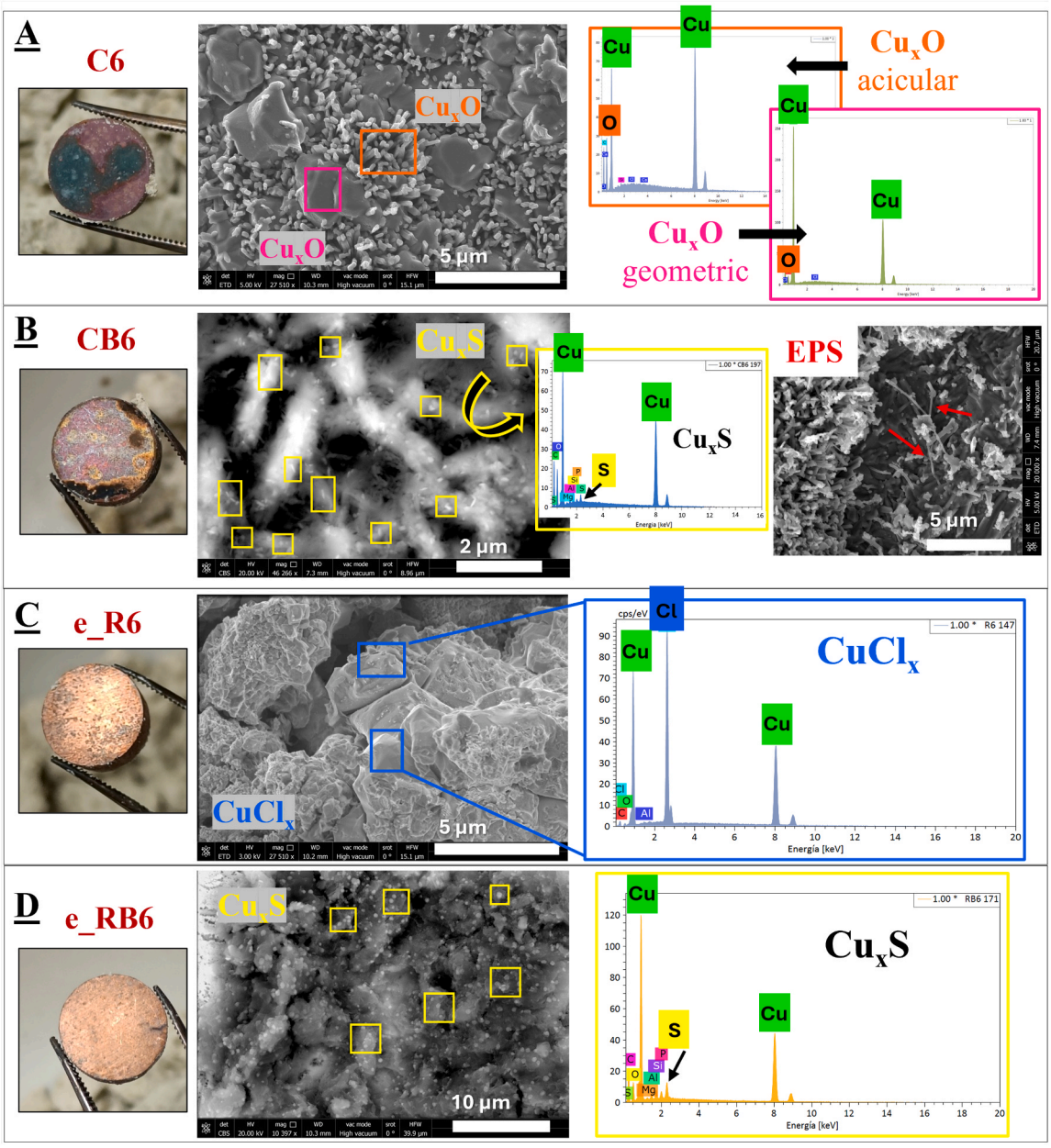

Fig. 4. Environmental scanning electron microscopy (ESEM) and energy dispersive X-ray (EDX) analysis of the copper disks corresponding to the 6-month incubation treatments. EDX spectra detail the signal of the elements that correspond to the main corrosion products together with Cu signal. Cu is represented in green, O in orange, S in yellow, and Cl in dark blue. **A.** C6 sample with Cu surface mainly covered by Cu_xO of different morphologies. **B.** CB6 sample showing small Cu-S precipitates within bentonite traces. EPS filaments are indicated with red arrows. **C.** e_R6 sample exhibiting copper chlorides precipitated between bentonite. **D.** e_RB6 sample exhibiting small Cu-S precipitates within bentonite traces.

radiation amended with SRB consortium (2RB12), these sulfur precipitates were not detected in the bentonite.

On the other hand, in all irradiated samples, regardless of consortium presence, Cu-S precipitates were observed to be located directly on the copper surface. These precipitates exhibited a distinct morphology and were larger in size compared to those observed in the bentonite (Fig. 5**C**). Additionally, copper chloride salts, which mainly precipitated between bentonite layers, were also found in almost all samples. The presence of chloride precipitates is likely attributable to the composition of the FEBEX pore water [12]. Fig. 4**C** showed the morphologies of these precipitated copper chlorides together with their EDX spectrum. In general, no bacterial cells were observed as biofilms on the copper surface. However, filamentous structures resembling extracellular polymeric substances (EPS) were detected in the unirradiated SRB consortium-amended samples at both 6 months and 1 year (CB6, CB12). An example of such EPS filaments (indicated by red arrows) found in CB6 copper disk sample is shown in Fig. 4**B**.

Furthermore, it should be noted that the Cu disks exhibiting minimal alterations based on surface corrosion products were those early irradiated with a dose of 14 kGy (e_R6, e_RB6) and those subjected to two irradiation exposure, accumulating a total dose of 28 kGy (2R12, 2RB12), as illustrated in Supplementary Figure S2. Interestingly, ESEM analysis confirmed the minimal alteration of these disks' surfaces, revealing certain areas with precipitates of Cu-O and Cu-S, as well as copper chlorides and traces of bentonite. In comparison to non-irradiated samples or those late irradiated, the presence of these corrosion products was greatly limited on most of the copper surface remaining unaltered. Supplementary Figure S4 illustrates the surfaces of

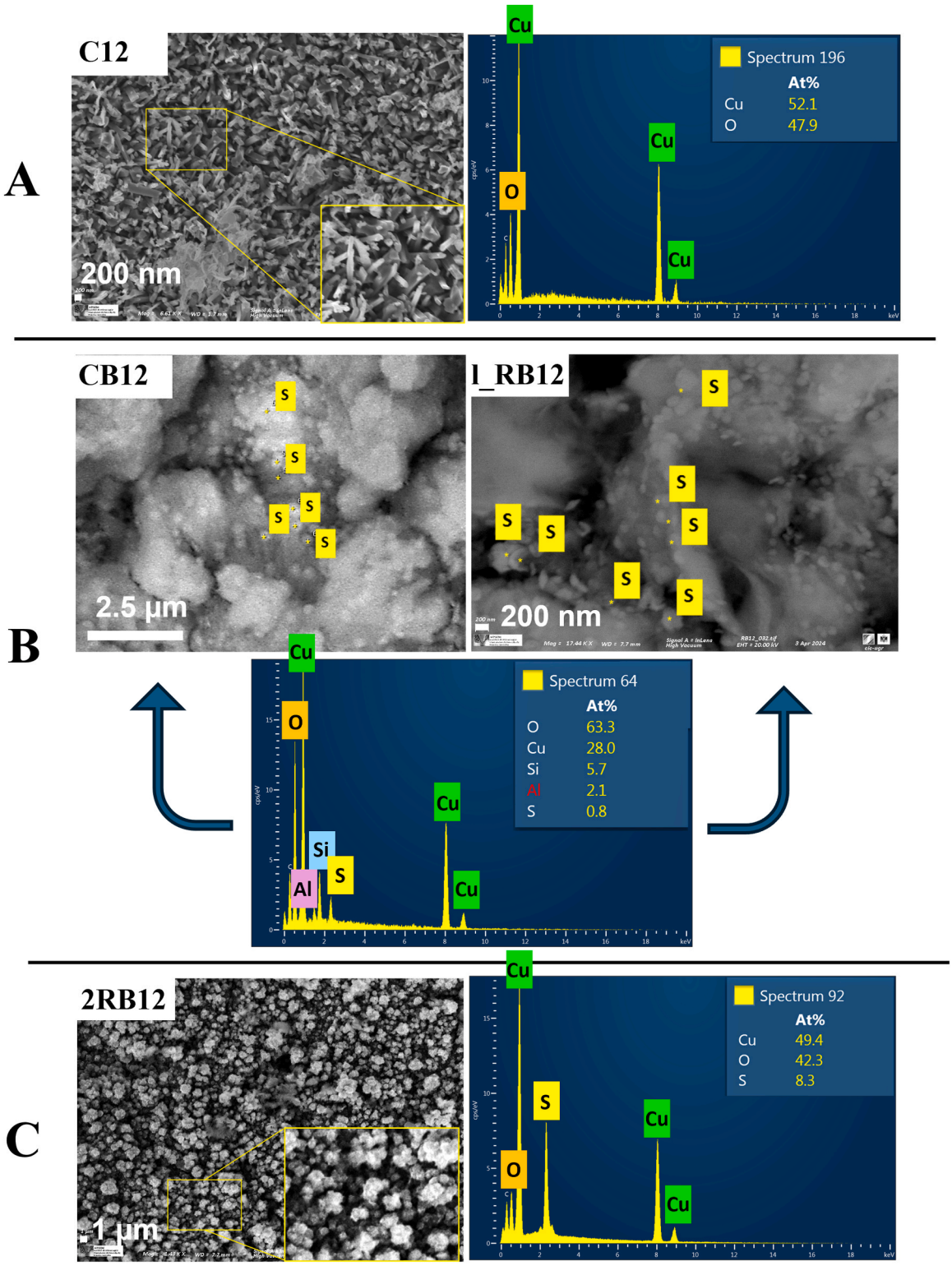

Fig. 5. Environmental scanning electron microscopy (ESEM) and energy dispersive X-ray (EDX) analysis of the copper disks corresponding to C12, CB12, l_RB12 and 2RB12 treatments after 1 year of incubation. **A.** C12 sample with Cu surface mainly covered by Cu_xO of different morphologies. **B.** CB12 and l_RB12 samples showing small Cu-S precipitates within bentonite traces. **C.** 2RB12 surface showing bigger Cu-S precipitates directly deposited on copper surface.

the Cu disks corresponding to the treatments after 6 months of incubation, showing a clear disparity in the amount of precipitated corrosion products.

To further assess and compare the surface composition of each Cu disk, X-ray photoelectron spectroscopy (XPS) analysis was performed. XPS spectra enabled identification of Cu-O and Cu-S precipitates previously observed by electron microscopy. Wide scans of the sample's surfaces revealed the presence of Cu, C, O, Si, Na, Fe, Mg and Al. Apart from copper, these elements most likely corresponded to bentonite adhering to the surface of the disks.

High-resolution scans conducted in the Cu 2p region (922–977 eV) for the untreated Cu control (Fig. 6) revealed a peak around 932.6 eV,

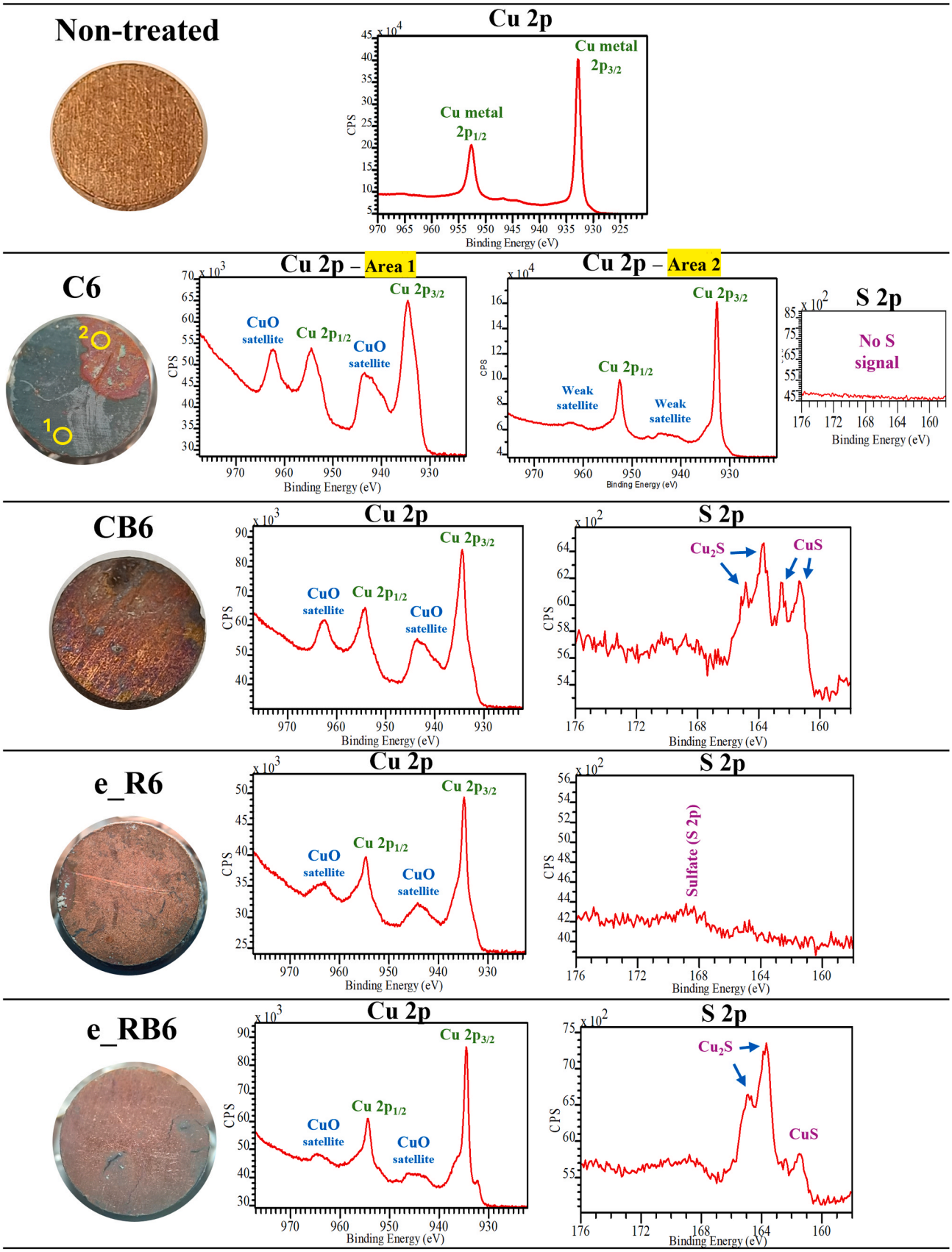

Fig. 6. High-resolution XPS spectra of the Cu 2p (977 eV – 922 eV) and S 2p (176 eV – 158 eV) regions of the Cu surface before experimental set-up (non-treated) and after 6 months of incubation.

consistent with reported values for elemental copper [35]. Conversely, CuO was found on all samples represented by satellite peaks around 939–942 eV (see Fig. 6 and Fig. 7)[35]. Furthermore, according to the literature, the peaks observed at 943.49 eV and 962.89 eV, and the distance between Cu $2p_{1/2}$ and Cu $2p_{3/2}$ peaks (19.96 eV) support the identification of CuO [36]. These peaks were not present in the untreated Cu control. Alongside this, area 2 on sample C6 (Fig. 6) demonstrated peaks at around 932.5 and 952.5 eV, which are commonly attributed to Cu_2O oxides [35]. Weak satellite peaks between ~939–948 eV and 957–965 eV suggest the presence of CuO on the surface, however less prominent than Cu_2O. After 12 months incubation, this treatment (C12) demonstrated strong satellite peaks representative of CuO, suggesting an oxidation of this area [35]. Under the anoxic incubation conditions presented in this study, it is expected that a Cu (I)-oxide should be the dominant species in the passive layer [37]. The indication of CuO by XPS, due to its highly surface sensitive nature, may only relate to a thin surface layer and not necessarily suggest the absence of Cu(I)-oxides. In addition to this, the overlap of Cu $2p_{3/2}$ peaks from Cu (0) and Cu(I) (932.6 ± 0.2 eV and 932.4 ± 0.2 eV, respectively) makes the distinction between Cu(0) and Cu(I) species from Cu 2p spectra uncertain [35]. This problem is further exacerbated as neither species (unlike CuO) demonstrate strong satellite peaks in the region around 939–945 eV.

The presence of Cu-S compounds in some of the Cu disks has been previously noted, highlighting small precipitates found within bentonite layers when the SRB consortium was present (CB6, e_RB6, CB12, l_RB12), and larger precipitates directly on the copper surface in all irradiated treatments (e_R6, e_RB6, l_R12, l_RB12, 2R12, 2RB12). XPS analyses of the Cu 2p spectra would elude identification of sulfur compounds present on copper surfaces. Krylova & Andrulevičius [38] reported that peaks corresponding to CuS typically appear at around 932.2 eV in high-resolution Cu 2p scans. However, if CuS were present, its peak would overlap with the copper oxides Cu $2p_{3/2}$ peak, thereby making its presence unable to be confirmed solely through the Cu 2p high-resolution spectrum. Therefore, in this study, high-resolution scans were also conducted in the S 2p region, within the range of 158–176 eV (Figs. 6 and 7). These XPS scans revealed the presence of sulfur on samples CB6, e_RB6, C12, CB12, 2R12 and 2RB12. More specifically, these samples showed peaks around 163 eV, which are related to the presence of Cu_2S [8,39]. Additionally, the peak observed at 161.4 eV was attributed to CuS according to Kutty [40]. In the irradiated samples, e_R6, 2R12 and 2RB12, a smooth peak was observed around 168.9 eV, which was attributed to the presence of sulfate [41], a compound present in the pore water.

In future facilities for nuclear waste emplaced 400–500 m in depth in geological formations, oxygen will only be present during the initial years after closure. Its availability will be gradually diminished due to predominant reducing conditions, bacterial activity and mineral oxidation [3]. Accordingly, in the present study, the assembly of the blocks was conducted in the presence of oxygen, but the incubation period was conducted under anoxic conditions. During the oxidizing period, it was possible that the copper may have undergone a spontaneous passivation process to protect its surface. Furthermore, Burzan et al. [29] reported the presence of oxygen molecules absorbed to bentonite mineral surfaces, thus creating microaerophilic environments. This, combined with the presence of pore water containing oxygen molecules in the samples, likely facilitated the formation of copper (II) oxides. In future highly compacted bentonite barriers, an initial degree of water saturation will be present, allowing some oxygen to persist as dissolved species. The most plausible reaction to be expected is the formation of copper(I) oxide, as described by the following equation $4Cu + O_2 \rightarrow 2Cu_2O$, reported by Hall et al. [42]. The copper oxides could continue to oxidize, resulting in the formation of copper(II) oxides, as evidenced by the XPS analysis (Figs. 6 and 7). This process could occur in a similar reaction as the one described by Mahmoodi et al. [43]: $2Cu_2O + O_2 \rightarrow 4CuO$.

On the other hand, one of the most critical sources of corrosion would be the production of sulfide by SRB. These microorganisms couple the oxidation of electron donors with the reduction of sulfate as the terminal electron acceptor [44,45] and are often responsible for MIC damage through the production of HS^-, which, when combined with H^+, forms H_2S. In future GDFs, bacteria would obtain electron donors from organic matter present in groundwater seepage, bentonite, or host rock, as well as from neighboring minerals. They may even utilize molecular hydrogen produced by the corrosion processes themselves. The viability of SRB was confirmed by the MPN results, while their proliferation during the incubation period was inferred from qPCR analysis. As mentioned above, SRB were generally present and viable in the non-irradiated treatments over time and were negatively affected by gamma irradiation. According to ESEM observations, bacterial cells were consistently associated with bentonite material adhering to the copper. Hall et al. [42] reported that microbial activity would mainly happen within the bentonite. The small S-containing precipitates localized between the bentonite layers in non-irradiated treatments inoculated with SRB consortium may have a biotic origin. This suggests that copper corrosion resulted from biogenic sulfide production, leading to the formation of copper sulfides, following the reaction: $2Cu + HS^- + H^+ \rightarrow Cu_2S\ (s) + H_2\ (g)$ [46]. These precipitates were observed only in treatments where SRB viability was confirmed, except for l_RB12. In this case, the sample was irradiated after 6 months of incubation, implying that sulfides formation likely occurred during the initial, nonirradiated phase, while subsequent radiation exposure reduced bacterial viability. Nevertheless, the presence of sulfides in this treatment could not be confirmed by XPS (Fig. 7).

On the other hand, XPS results did confirm the presence of Cu_2S in all those treatments corresponding to 6 months (CB6, e_RB6) and 1 year (CB12, 2RB12) of anoxic incubation. Since all these treatments involved SRB consortium, these results support the ability of such bacteria to form copper sulfides under conditions relevant to GDFs. Surprisingly, the treatment 2R12, which was not inoculated with the SRB consortium, also displayed sulfide peaks in the XPS spectra (Fig. 7). However, based on the microbiological results reported by Morales-Hidalgo et al. [12] and in the present study, no bacterial viability or activity was detected in this double-irradiated treatment, suggesting that the observed sulfide formation likely resulted from an abiotic process. Furthermore, the Cu disk samples from 2R12 and 2RB12 treatments were the only ones exposed to the highest accumulated radiation dose of 28 kGy. In both cases, this elevated radiation level may have had a dual effect: on one hand, effectively reducing biotic corrosion by eliminating microbial activity; on the other, potentially enhancing abiotic corrosion processes. Although the exact mechanism remains unclear, previous studies under different conditions suggest that gamma radiation can induce the formation of sulfur-based radicals from sulfate compounds, which may subsequently be reduced to H_2S [47,48]. The resulting H_2S could then react with copper or its oxides, leading to the precipitation of copper sulfides such as CuS or Cu_2S.

Additionally, larger S-containing precipitates were also detected directly on the copper surface in all irradiated treatments, regardless of the presence of the SRB consortium. Li et al. [49] reported that γ-radiation induced synthesis involving redox reactions between water radiolysis products, radicals and active species, and dissolved metal salt precursors, resulting in the precipitation of low-solubility compounds. Moreover, as noted by Hall et al. [42], groundwater in a GDF environment is expected to contain various anions resulting from host rock mineral dissolution, particularly chloride, sulfate, and carbonate. Therefore, the present work suggests the formation of copper salts incorporating these anions, such as the observed copper sulfate and copper chloride, is likely under such conditions.

The formation of these copper sulfides is expected to occur during the early stages of dominant reducing conditions, once available oxygen has been fully depleted and the oxic corrosion phase has ended. At that point, sulfide production by SRB under anaerobic conditions is likely to

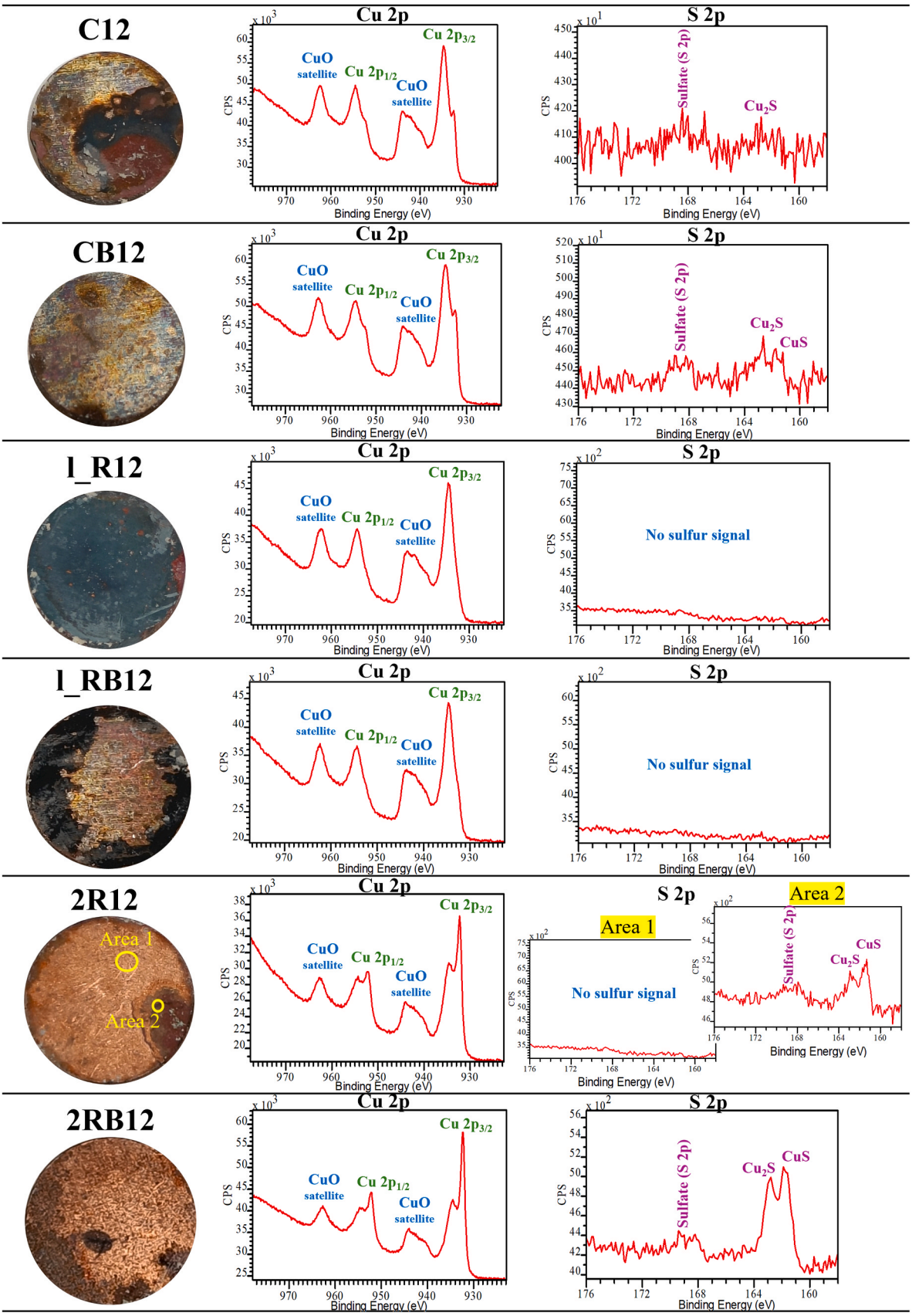

Fig. 7. High-resolution XPS spectra of the Cu 2p (977 eV – 922 eV) and S 2p (176 eV – 158 eV) regions of the Cu surface after 1 year of incubation.

result in interactions with copper surfaces already coated with corrosion-derived oxide layers. The transformation of Cu_2O to Cu_2S has been documented by Smith et al. [50]. Accordingly, these oxide layers may serve as a protective barrier against sulfide-induced corrosion, as the sulfides would primarily react with existing corrosion products rather than with metallic copper itself [42].

Ensuring the long-term safety of future nuclear repositories is essential for the protection of the biosphere. Consequently, every component of the multisystem must be carefully designed and rigorously evaluated to guarantee the stability of the GDFs over timescales as long as the estimated 100,000 years. A critical component of this system is the metallic canister that contains radioactive waste, which must remain as intact as possible throughout this extended period. This study focused on the alteration of copper, a candidate material for canisters in

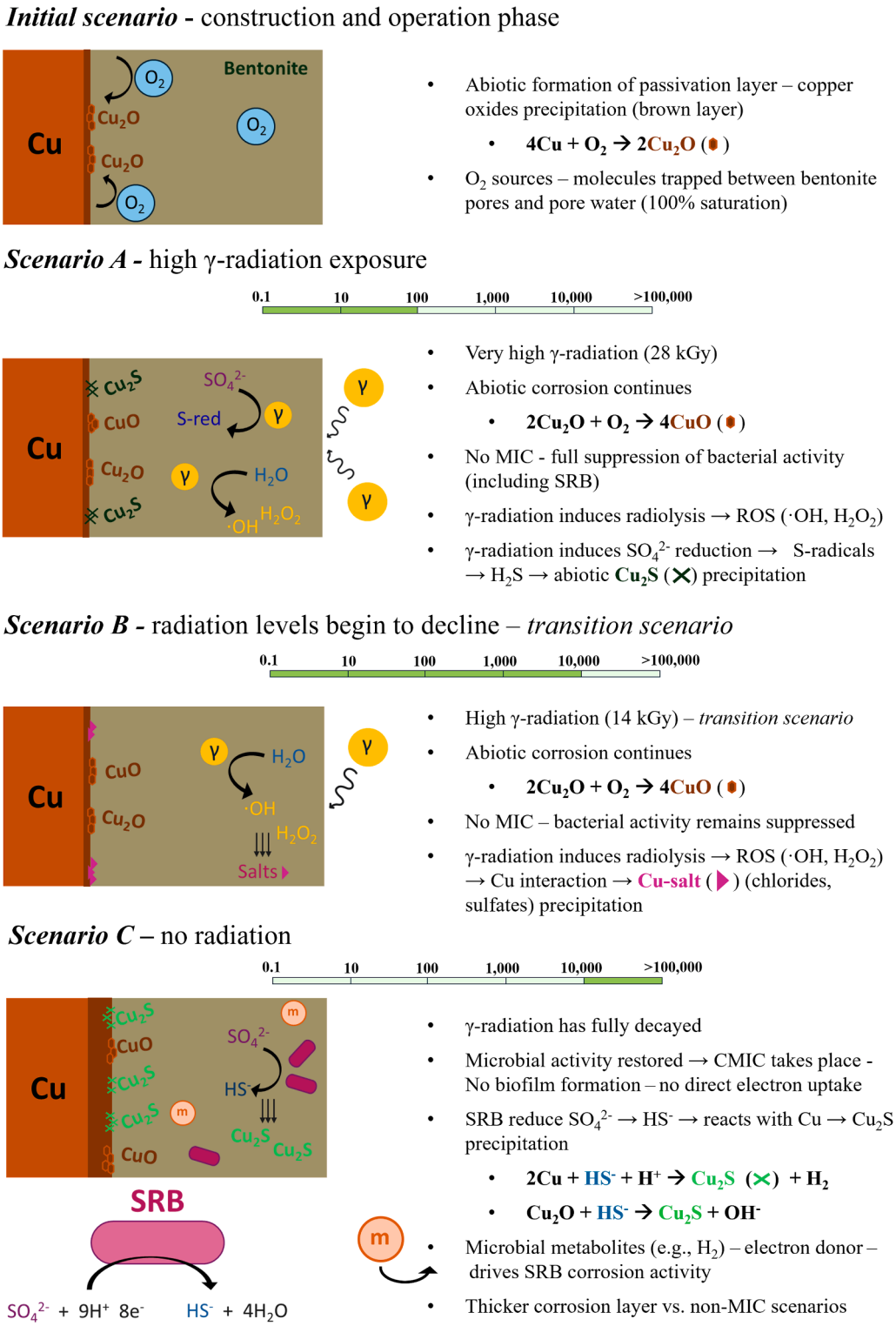

Fig. 8. Conceptual scheme illustrating the hypothetical mechanisms of copper corrosion product formation and transformation across the successive stages of a GDF lifetime. ROS: reactive oxygen species; MIC: microbially influenced corrosion; CMIC: chemical MIC.

countries such as Finland and Sweden [5]. In general, copper can be altered by a variety of physical, chemical, and biological factors, including the presence of water, radiation exposure, and microbial activity, among others. The results presented here have important implications for the environmental safety of GDFs. Gamma radiation was found to significantly reduce the viability of SRB, which are major contributors to microbially influenced corrosion of copper canisters. This implies that during the early stages of repository operation, when radiation levels are highest, biotic corrosion of copper is likely to be minimal, thereby lowering the risk of early canister alteration. In addition, the study showed that copper corrosion under the tested conditions primarily led to the formation of copper oxides, and that radiation may delay microbial corrosion mechanisms. These findings underscore the importance of thoroughly understanding the interplay between radiation, microbial activity, and bentonite compaction in shaping the long-term performance and environmental safety of nuclear waste storage systems.

3.4. Hypothetical Cu corrosion mechanisms over GDF timescales: a schematic approach

The findings obtained in this study have enabled the development of a conceptual model describing how MIC may occur at the copper–compacted bentonite interface under irradiated repository conditions.

Based on the results obtained and supported by existing knowledge on copper corrosion in repository-relevant environments [42], a schematic model has been developed to illustrate the potential mechanisms of copper corrosion within a GDF (Fig. 8). The proposed model delineates four sequential phases consistent with the established timeline of a GDF lifetime [3,51]. The first phase represents the *initial scenario*, a stage common to all experimental conditions examined. This phase corresponds to the early operational years of the repository, during which oxic conditions prevail. Over this period, the repository will be gradually filled until completion and definitive closure is achieved. In the context of the present experiment, this stage reflects the period when the copper disks were predominantly exposed to oxic conditions during block assembly. Oxygen molecules may also have been trapped within the bentonite pore network and adsorbed onto clay minerals [29]. Together with the added pore water, this contributed to the persistence of oxygen at the Cu–bentonite interface. Consequently, an early passivation layer was formed on the copper surfaces during the initial incubation period across all Cu samples. This layer was initially composed of Cu(I) oxides, which gradually oxidizes to Cu(II) oxides over time.

The subsequent phase, referred to as *Scenario A*, corresponds to conditions of high gamma radiation exposure (samples subjected to double irradiation, with a total accumulated dose of 28 kGy). This scenario represents the first decades of repository operation, during which radiation emitted by the waste is expected to reach its maximum intensity [51]. In the doubly irradiated treatments, only the copper oxide passivation layer was formed, which would continue to develop over time due to abiotic corrosion processes. Furthermore, gamma radiation exposure is known to induce water radiolysis, generating reactive oxygen species (ROS) such as hydroxyl radicals (·OH) and hydrogen peroxide (H_2O_2). These oxidizing agents can additionally enhance the oxidative dissolution of metallic copper ($Cu^0 \rightarrow Cu^+ \rightarrow Cu^{2+}$), thereby promoting the transformation of the Cu(I)-dominated passive layer into Cu(II) oxides. In addition, ROS may interact with copper at the Cu–bentonite interface, potentially leading to the precipitation of copper salts, including sulfates and chlorides (e.g., $CuSO_4 \cdot xH_2O$ and $CuCl_2 \cdot xH_2O$), which were detected in all irradiated samples. The presence of moisture from the added pore water would facilitate ion mobility and precipitation-dissolution processes, enabling these reactions. At this stage, microbial activity, including that of SRB, is assumed to be completely suppressed, meaning that all corrosion processes are considered to proceed via abiotic mechanisms. This statement is supported by the viability data (Table 1) presented in this study, where no SRB viability was observed in most irradiated treatments. Considering that MIC processes are inhibited under these conditions, it is hypothesized that gamma radiation may generate sulfur-based radicals through the radiolysis of sulfate species present in the pore water [47,48]. These radicals could subsequently yield reduced hydrogen sulfide (H_2S), which may react with copper or copper oxides, potentially leading to the formation of copper sulfides (Cu_2S). Such sulfide precipitates were identified by XPS in the 28 kGy-irradiated samples (2R12, 2RB12).

As a transitional phase, *Scenario B* corresponds to treatments exposed to 14 kGy — a high radiation dose, though lower than that of *Scenario A*. This scenario represents a later stage in the repository's lifetime (hundreds of years), during which radiation levels are expected to begin to decline [51]. At this dose, SRB activity is assumed to remain suppressed, and consequently, MIC processes are not expected to affect the copper material or surface. Consistent with the previous scenario, the corrosion product layer is assumed to consist of a passivation layer accompanied by copper oxides precipitated through abiotic corrosion. However, for these disks, corrosion layer growth is anticipated to be minimal, and surface damage is predicted to remain limited. At this dose of 14 kGy, the reduced radiation leads to a lower steady-state concentration of ROS; nonetheless, ROS generation would still occur, potentially contributing to abiotic copper oxidation reactions and the precipitation of copper salts, thereby reinforcing the passive barrier. Mechanistically, *Scenario B* can be interpreted as a quasi-steady-state regime in which the corrosion kinetics transition from radiation-enhanced oxidation toward diffusion-controlled passive behavior.

The final phase, *Scenario C*, represents the most advanced stage of the repository, in which radiation has fully decayed and no residual radiation remains [51]. Representative samples for this scenario are the non-irradiated controls: C6, CB6, C12, and CB12. Under these conditions, microbial activity could be restored, and MIC processes are expected to take place. The formation of both Cu(I) and Cu(II) oxides can occur due to pore water acting as an electrolyte and microbial metabolism altering local redox conditions, thereby favoring copper oxidation and precipitation. Specifically, SRB would reduce sulfate present in the pore water to sulfide, which can react with copper, leading to the precipitation of copper sulfides. This is supported by the XPS spectra of samples CB6 and CB12, in which the SRB consortium was present, and the activity of these bacteria was predominantly reflected, resulting in the detection of biogenic copper sulfides. Sulfate reduction may be further enhanced by the metabolic by-products of other viable microbial groups, such as *Clostridium*. This genus, present as a native member of FEBEX and viable in most SRB-positive treatments (Fig. 3), can produce hydrogen (H_2) and other metabolites such as acetate through microbial fermentation, serving as additional electron donors and promoting bacterial sulfate reduction. These processes are envisaged to occur under compacted bentonite conditions (1.6 g/cm^3), where molecular diffusion is strongly hindered but not completely prevented. Under these circumstances, a cathodic depolarization mechanism may also operate, since hydrogen generated at the copper surface during proton reduction could be removed from the bulk by SRB located within the bentonite matrix. As no biofilm is formed directly on the copper surface, MIC would proceed heterogeneously, with copper sulfide precipitation restricted to areas where reduced sulfur species (HS^- or H_2S), produced by SRB activity, are able to diffuse and reach the metal interface. Since sulfide species are relatively small, their diffusion capacity through the compacted bentonite to the canister surface is expected to be limited but achievable [52]. Furthermore, although these engineering barriers will restrict the amount of "free" pore water, this will be still available within bentonite pores, as well as through microchannels and small fractures within the bentonite blocks, providing pathways for both reduced sulfur species and possibly hydrogen to migrate within the compacted clay and influence copper corrosion.

In the conceptual model proposed here, direct electron uptake by

SRB is not considered. Instead, the mechanism corresponds to a chemical MIC (CMIC), in which corrosion is indirectly driven by the action of microbial metabolic by-products. In this case, reduced sulfur species produced during SRB metabolism diffuse through the compacted bentonite and chemically react with copper at the interface, resulting in copper sulfide precipitation. In contrast, electrical MIC (EMIC) involves the direct uptake of electrons from the metal by bacterial cells. This mechanism is commonly associated with other microorganisms, such as iron-reducing bacteria, and with metals such as carbon steel. Moreover, EMIC typically requires the formation of a biofilm directly attached to the metal surface, a condition excluded from this model due to the inherent toxicity of copper to bacteria.

4. Conclusions and future scope

This study provides the first combined assessment of microbiology and copper corrosion under gamma radiation exposure in compacted bentonite systems, directly addressing conditions relevant to GDFs. This integrative approach is novel, as previous research has typically considered microbial activity, corrosion processes, or radiation effects separately.

These results showed that gamma radiation at cumulative doses $\geq$ 14 kGy (0.66 Gy/h) substantially reduces SRB viability, indicating that these microorganisms are unlikely to contribute to MIC during the initial centuries of GDF operation, when radiation fields are at their maximum. Copper corrosion was instead dominated by oxide formation (mainly CuO), with oxygen sources attributed to bentonite compaction procedure, adsorbed molecules, or pore water. Radiation further delayed biotic corrosion by suppressing microbial populations and promoting the precipitation of salts, including potential copper sulfates. In later repository stages, when radiation decays, SRB activity may resume, producing biogenic copper sulfides. Importantly, this work confirmed that SRB activity would be restricted to bentonite-containing zones, which narrows the spatial domain of potential MIC.

Overall, these findings significantly advance current understanding by clarifying both the temporal and spatial interplay of radiation, bentonite, and microbial processes. The results demonstrated that (i) gamma radiation initially protects copper canisters by suppressing SRB activity, (ii) microbial contributions to corrosion are more relevant in the long-term evolution of the repository, and (iii) SRB-driven corrosion is confined to bentonite environments. By integrating microbiological, radiological, and geochemical perspectives under repository-relevant conditions, this study strengthens the scientific basis for assessing canister durability and the safety functions of GDF design.

CRediT authorship contribution statement

Mar Morales-Hidalgo: Writing – review & editing, Writing – original draft, Visualization, Validation, Methodology, Investigation, Formal analysis, Data curation, Conceptualization. **Cristina Povedano-Priego:** Writing – review & editing, Validation, Methodology, Conceptualization. **Marcos F. Martinez-Moreno:** Writing – review & editing, Validation, Investigation. **Adam D. Mumford:** Writing – review & editing, Validation, Investigation, Formal analysis. **Kateřina Černá:** Writing – review & editing, Validation, Resources, Formal analysis. **Yon Ju-Nam:** Writing – review & editing, Validation. **Jesus J. Ojeda:** Writing – review & editing, Validation, Resources. **Ana María Fernández:** Validation, Methodology, Conceptualization. **Ursula Alonso:** Writing – review & editing, Validation, Resources, Methodology, Conceptualization. **Fadwa Jroundi:** Writing – review & editing, Validation, Supervision, Methodology, Conceptualization. **Mohamed L. Merroun:** Writing – review & editing, Visualization, Validation, Supervision, Resources, Project administration, Methodology, Funding acquisition, Conceptualization.

Funding

This research was co-funded by the European Union's Horizon 2020 research and innovation programme under grant agreements N° 847593 (EURAD-1) and N° 101166718 (EURAD-2). In addition, this work has also been partially supported by Funding from the Spanish Ministry of Science, Innovation and Universities (MCIN/AEI/10.13039/501100011033) through the ACOMER Project PID2022–138402NB-C21 and PID2022–138402NB-C22. The grant FPU20/00583 from "Ministerio de Universidades" to the first author from the Spanish Government is also acknowledged, as well as support from the EURAD Mobility Programme for the award of a Research and Training Grant at the Technical University of Liberec (Czech Republic). Additional financial contributions came from SÚRAO (SO2020–017). ADM acknowledges funding from the UK Engineering and Physical Sciences Research Council (EPSRC) DTP scholarship (project reference: 2748843). Funding for open access charge: Universidad de Granada / CBUA.

Declaration of Competing Interest

The authors declare that they have no known competing financial interests or personal relationships that could have appeared to influence the work reported in this paper.

Acknowledgements

The authors acknowledge the assistance of Pedro Valdivieso for his assistance in the radioactive installations of the Nayade facility of CIEMAT. The authors also thank Manuel Mingarro and Jesús Morejón for their help with sample preparation at CIEMAT and Dr. Isabel Guerra-Tschuschke (CIC, University of Granada) for microscopy support.

Appendix A. Supporting information

Supplementary data associated with this article can be found in the online version at doi:10.1016/j.corsci.2025.113443.

Data availability

Data will be made available on request.

References

[1] IAEA, Status and trends in spent fuel and radioactive waste management. Vienna, international atomic energy agency, in: Nuclear Energy Series No. NW-T-1, 14, 2018. ⟨https://www-pub.iaea.org/MTCD/Publications/PDF/PUB1963_web.pdf⟩ (Available at).

[2] M. Morales-Hidalgo, C. Povedano-Priego, M.F. Martinez-Moreno, M.A. Ruiz-Fresneda, M. Lopez-Fernandez, F. Jroundi, M.L. Merroun, Insights into the impact of physicochemical and microbiological parameters on the safety performance of deep geological repositories, Microorganisms 12 (2024) 1025, https://doi.org/10.3390/microorganisms12051025.

[3] F. King, D.S. Hall, P.G. Keech, Nature of the near-field environment in a deep geological repository and the implications for the corrosion behaviour of the container, Corros. Eng. Sci. Technol. 52 (2017) 25–30, https://doi.org/10.1080/1478422X.2017.1330736.

[4] M. Jonsson, G. Emilsson, L. Emilsson, Mechanical design analysis for the canister, Posiva SKB Rep. 4 (2018) 147 (n.d).

[5] D.G. Bennett, R. Gens, Overview of european concepts for high-level waste and spent fuel disposal with special reference waste container corrosion, J. Nucl. Mater. 379 (2008) 1–8, https://doi.org/10.1016/j.jnucmat.2008.06.001.

[6] A. Abdelouas, U. Alonso, R. Bernier-Latmani, C. Bosch, A. Cherkouk, D. Dobrev, A. M. Fernández, N. Finck, R. Gaggiano, V. Havlová, et al., Initial State-of-the-Art of WP ConCorD. Final Version as of 17.08.2022 of Deliverable D15.1 of the HORIZON 2020 Project EURAD; EC Grant agreement no: 847593. (2022). Available online: ⟨https://www.ejp-eurad.eu/sites/default/files/2022-09/EURAD%20-%20D15.1%20ConCorD%20Initial%20SotA.pdf⟩.

[7] M.A. Ruiz-Fresneda, M.F. Martinez-Moreno, C. Povedano-Priego, M. Morales-Hidalgo, F. Jroundi, M.L. Merroun, Impact of microbial processes on the safety of deep geological repositories for radioactive waste, Front. Microbiol. 14 (2023) 1134078, https://doi.org/10.3389/fmicb.2023.1134078.

[8] M.F. Martinez-Moreno, C. Povedano-Priego, M. Morales-Hidalgo, A.D. Mumford, J. J. Ojeda, F. Jroundi, M.L. Merroun, Impact of compacted bentonite microbial

community on the clay mineralogy and copper canister corrosion: a multidisciplinary approach in view of a safe deep geological repository of nuclear wastes, J. Hazard. Mater. 458 (2023) 131940, https://doi.org/10.1016/j.jhazmat.2023.131940.
[9] M.F. Martinez-Moreno, C. Povedano-Priego, A.D. Mumford, M. Morales-Hidalgo, K. Mijnendonckx, F. Jroundi, J.J. Ojeda, M.L. Merroun, Microbial responses to elevated temperature: evaluating bentonite mineralogy and copper canister corrosion within the long-term stability of deep geological repositories of nuclear waste, Sci. Total Environ. 915 (2024) 170149, https://doi.org/10.1016/j.scitotenv.2024.170149.
[10] H.M. Haynes, C.I. Pearce, C. Boothman, J.R. Lloyd, Response of bentonite microbial communities to stresses relevant to geodisposal of radioactive waste, Chem. Geol. 501 (2018) 58–67, https://doi.org/10.1016/j.chemgeo.2018.10.004.
[11] E. García-Romero, E. María Manchado, M. Suárez, J. García-Rivas, Spanish bentonites: a review and new data on their geology, mineralogy, and crystal chemistry, Minerals 9 (2019) 696, https://doi.org/10.3390/min9110696.
[12] M. Morales-Hidalgo, C. Povedano-Priego, M.F. Martinez-Moreno, K. Černá, K. Lísková, J. Říha, P. Valdivieso, U. Alonso, A.M. Fernández, F. Jroundi, M. L. Merroun, Gamma radiation in highly compacted FEBEX bentonite: key microbial and mineralogical behavior for safety assessment of nuclear repositories, J. Hazard. Mater. 495 (2025) 138915, https://doi.org/10.1016/j.jhazmat.2025.138915.
[13] M. Jonsson, Radiation effects on materials used in geological repositories for spent nuclear fuel, ISRN Mater. Sci. (2012) 1–13, https://doi.org/10.5402/2012/639520.
[14] D. Bartak, E. Bedrníková, V. Kašpar, J. Říha, V. Hlaváčková, P. Večerník, Š. Šachlová, K. Černá, Survivability and proliferation of microorganisms in bentonite with implication to radioactive waste geological disposal: strong effect of temperature and negligible effect of pressure, World J. Microbiol. Biotechnol. 40 (2024) 41, https://doi.org/10.1007/s11274-023-03849-0.
[15] D. Bartak, J. Říha, D. Dudáš, P. Gallus, E. Bedrníková, V. Kašpar, K. Černá, Bentonite sterilization methods in relation to geological disposal of radioactive waste: comparative efficiency of dry heat and gamma radiation, J. Appl. Microbiol. 136 (2025) lxaf051, https://doi.org/10.1093/jambio/lxaf051.
[16] F. Huertas, J.L. Fuentes-Santillana, F. Jullien, P. Rivas, J. Linares, P. Fariña, M. Ghoreychi, N. Jockwer, W. Kickmaier, M.A. Martínez, J. Samper, E. Alonso, F. J. Elorza, Full scale engineered barriers experiment for a deep geological repository for high-level radioactive waste in crystalline host rock, EC Final Rep. EUR 19147 (2020).
[17] A.M. Fernández, B. Baeyens, M. Bradbury, P. Rivas, Analysis of the porewater chemical composition of a spanish compacted bentonite used in an engineered barrier, Phys. Chem. Earth Parts A/B/C. 29 (2004) 105–118, https://doi.org/10.1016/j.pce.2003.12.001.
[18] A.M. Fernandez, P. Rivas, in: Alonso, Ledesma (Eds.), Pore water chemistry of saturated FEBEX bentonite compacted at different densities. Advances in Understanding Engineered Barriers, Taylor and Francis Group, London, 2005, pp. 505–514. ISBN 04-1536-544-9., (n.d.).
[19] M. Guo, The electrochemical and corrosion study of copper for nuclear waste containers under deep geological disposal conditions, (Doctoral Dissertation, The University of Western Ontario, Canada, 2020.
[20] M. Morales-Hidalgo, C. Povedano-Priego, M.F. Martinez-Moreno, J.J. Ojeda, F. Jroundi, M.L. Merroun, Long-term tracking of the microbiology of uranium-amended water-saturated bentonite microcosms: a mechanistic characterization of u speciation, J. Hazard. Mater. 476 (2024) 135044, https://doi.org/10.1016/j.jhazmat.2024.135044.
[21] C. Povedano-Priego, F. Jroundi, M. Lopez-Fernandez, M. Morales-Hidalgo, I. Martin-Sánchez, F.J. Huertas, M. Dopson, M.L. Merroun, Impact of anoxic conditions, uranium(VI) and organic phosphate substrate on the biogeochemical potential of the indigenous bacterial community of bentonite, Appl. Clay Sci. 216 (2022) 106331, https://doi.org/10.1016/j.clay.2021.106331.
[22] C. Povedano-Priego, F. Jroundi, M. Lopez-Fernandez, R. Shrestha, R. Spanek, I. Martín-Sánchez, M.V. Villar, A. Ševců, M. Dopson, M.L. Merroun, Deciphering indigenous bacteria in compacted bentonite through a novel and efficient DNA extraction method: insights into biogeochemical processes within the deep geological disposal of nuclear waste concept, J. Hazard. Mater. 408 (2021) 124600, https://doi.org/10.1016/j.jhazmat.2020.124600.
[23] R. Shrestha, K. Cerna, R. Spanek, D. Bartak, T. Cernousek, A. Sevcu, The effect of low-pH concrete on microbial community development in bentonite suspensions as a model for microbial activity prediction in future nuclear waste repository, Sci. Total Environ. 808 (2022) 151861, https://doi.org/10.1016/j.scitotenv.2021.151861.
[24] O. Lhotský, J. Kukačka, J. Slunský, K. Marková, J. Němeček, V. Knytl, T. Cajthaml, The effects of hydraulic/pneumatic fracturing-enhanced remediation (FRAC-IN) at a site contaminated by chlorinated ethenes: a case study, J. Hazard. Mater. 417 (2021) 125883, https://doi.org/10.1016/j.jhazmat.2021.125883.
[25] R. Shrestha, T. Černoušek, J. Stoulil, H. Kovářová, K. Sihelská, R. Špánek, A. Ševců, J. Steinová, Anaerobic microbial corrosion of carbon steel under conditions relevant for deep geological repository of nuclear waste, Sci. Total Environ. 800 (2021) 149539, https://doi.org/10.1016/j.scitotenv.2021.149539.
[26] T.F. Anderson, Techniques for the preservaation of three-dimensional structure in preparing specimens for the electron microscope*, Trans. NY Acad. Sci. 13 (1951) 130–134, https://doi.org/10.1111/j.2164-0947.1951.tb01007.x.
[27] N. Fairley, V. Fernandez, M. Richard-Plouet, C. Guillot-Deudon, J. Walton, E. Smith, D. Flahaut, M. Greiner, M. Biesinger, S. Tougaard, D. Morgan, J. Baltrusaitis, Systematic and collaborative approach to problem solving using X-ray photoelectron spectroscopy, Appl. Surf. Sci. Adv. 5 (2021) 100112, https://doi.org/10.1016/j.apsadv.2021.100112.
[28] K. Pedersen, Analysis of copper corrosion in compacted bentonite clay as a function of clay density and growth conditions for sulfate-reducing bacteria, J. Appl. Microbiol. 108 (2010) 1094–1104, https://doi.org/10.1111/j.1365-2672.2009.04629.x.
[29] N. Burzan, R. Murad Lima, M. Frutschi, A. Janowczyk, B. Reddy, A. Rance, N. Diomidis, R. Bernier-Latmani, Growth and persistence of an aerobic microbial community in Wyoming bentonite MX-80 despite anoxic in situ conditions, Front. Microbiol. 13 (2022) 858324, https://doi.org/10.3389/fmicb.2022.858324.
[30] A. Bengtsson, K. Pedersen, Microbial sulphide-producing activity in water saturated Wyoming MX-80, asha and calcigel bentonites at wet densities from 1500 to 2000 kgm^{-3}, Appl. Clay Sci. 137 (2017) 203–212, https://doi.org/10.1016/j.clay.2016.12.024.
[31] M.F. Martinez-Moreno, C. Povedano-Priego, M. Morales-Hidalgo, A.D. Mumford, G. Lazuen-Lopez, E. Aranda, R. Vilchez-Vargas, P.L. Solari, Y. Ju-Nam, F. Jroundi, J.J. Ojeda, M.L. Merroun, Dual effect of Se(IV) and bentonite microbial community interactions on the corrosion of copper and se speciation: implication on repository safety assessment, Sci. Total Environ. 965 (2025) 178613, https://doi.org/10.1016/j.scitotenv.2025.178613.
[32] M. Watanabe, H. Kojima, M. Fukui, Review of *desulfotomaculum* species and proposal of the genera *desulfallas* gen. Nov., *desulfofundulus* gen. Nov., *desulfofarcimen* gen. Nov. and *desulfohalotomaculum* gen. Nov, Int. J. Syst. Evol. Microbiol. 68 (2018) 2891–2899, https://doi.org/10.1099/ijsem.0.002915.
[33] L.L. Campbell, Jr, H.A. Frank, E.R. Hall, Studies on thermophilic sulfate reducing bacteria I. *sporovibrio desulfuricans* as *clostridium nigrificans*, J. Bacteriol. 73 (1957) 516–521.
[34] I. Tang, M.R. Okos, S. Yang, Effects of ph and acetic acid on homoacetic fermentation of lactate by *clostridium formicoaceticum*, Biotech. BME 34 (1989) 1063–1074, https://doi.org/10.1002/bit.260340807.
[35] M.C. Biesinger, Advanced analysis of copper X-ray photoelectron spectra, Surf. Interface Anal. 49 (2017) 1325–1334, https://doi.org/10.1002/sia.6239.
[36] C.D. Wagner, W.M. Riggs, L.E. Davis, J.F. Moulder, G.E. Muilenberg, Handbook of X-ray photoelectron spectroscopy: a reference book of standard data for use in X-ray photoelectron spectroscopy. (1979) Perkin-Elmer Corporation: Eden Prairie, MN, n.d.
[37] F. King, M. Behazin, A review of the effect of irradiation on the corrosion of copper-coated used fuel containers, CMD 2 (2021) 678–707, https://doi.org/10.3390/cmd2040037.
[38] V. Krylova, M. Andrulevičius, Optical, XPS and XRD studies of semiconducting copper sulfide layers on a polyamide film, Int. J. Photo (2009) 304308, https://doi.org/10.1155/2009/304308.
[39] X.-R. Yu, F. Liu, Z.-Y. Wang, Y. Chen, Auger parameters for sulfur-containing compounds using a mixed aluminum-silver excitation source, J. Electron Spectrosc. Relat. Phenom. 50 (1990) 159–166, https://doi.org/10.1016/0368-2048(90)87059-W.
[40] T.R.N. Kutty, A controlled copper-coating method for the preparation of ZnS: mn DC electroluminescent powder phosphors, Mater. Res. Bull. 26 (1991) 399–406, https://doi.org/10.1016/0025-5408(91)90054-P.
[41] Y. Cai, Y. Pan, J. Xue, Q. Sun, G. Su, X. Li, Comparative XPS study between experimentally and naturally weathered pyrites, Appl. Surf. Sci. 255 (2009) 8750–8760, https://doi.org/10.1016/j.apsusc.2009.06.028.
[42] D.S. Hall, M. Behazin, W. Jeffrey Binns, P.G. Keech, An evaluation of corrosion processes affecting copper-coated nuclear waste containers in a deep geological repository, Prog. Mater. Sci. 118 (2021) 100766, https://doi.org/10.1016/j.pmatsci.2020.100766.
[43] A. Mahmoodi, S. Solaymani, M. Amini, N.B. Nezafat, M. Ghoranneviss, Structural, morphological and antibacterial characterization of CuO nanowires, Silicon 10 (2018) 1427–1431, https://doi.org/10.1007/s12633-017-9621-2.
[44] B.J. Little, J. Hinks, D.J. Blackwood, Microbially influenced corrosion: towards an interdisciplinary perspective on mechanisms, Int. Biodeterior. Biodegrad 154 (2020) 105062, https://doi.org/10.1016/j.ibiod.2020.105062.
[45] R.K. Thauer, E. Stackebrandt, W.A. Hamilton, Energy metabolism and phylogenetic diversity of sulphate-reducing bacteria, in: L.L. Barton, W.A. Hamilton (Eds.), Sulphate-Reducing Bacteria, 1st ed, Cambridge University Press, 2007, pp. 1–38, https://doi.org/10.1017/CBO9780511541490.002.
[46] E. Huttunen-Saarivirta, P. Rajala, L. Carpén, Corrosion behaviour of copper under biotic and abiotic conditions in anoxic ground water: electrochemical study, Electrochim. Acta 203 (2016) 350–365, https://doi.org/10.1016/j.electacta.2016.01.098.
[47] J.D. Cope, K.H. Bates, L.N. Tran, K.A. Abellar, T.B. Nguyen, Sulfur radical formation from the tropospheric irradiation of aqueous sulfate aerosols, Proc. Natl. Acad. Sci. U. S. A. 119 (2022) e2202857119, https://doi.org/10.1073/pnas.2202857119.
[48] M. Bekhit, A.O. Abo El Naga, M. El Saied, M.I.A. Abdel Maksoud, Radiation-induced synthesis of copper sulfide nanotubes with improved catalytic and antibacterial activities, Environ. Sci. Pollut. Res 28 (2021) 44467–44478, https://doi.org/10.1007/s11356-021-13482-9.
[49] Z. Li, Y. Yang, A. Relefors, X. Kong, G.M. Siso, B. Wickman, Y. Kiros, I.L. Soroka, Tuning morphology, composition and oxygen reduction reaction (ORR) catalytic performance of manganese oxide particles fabricated by γ-radiation induced synthesis, J. Colloid Interface Sci. 583 (2021) 71–79, https://doi.org/10.1016/j.jcis.2020.09.011.

[50] J.M. Smith, J.C. Wren, M. Odziemkowski, D.W. Shoesmith, The electrochemical response of preoxidized copper in aqueous sulfide solutions, J. Electrochem. Soc. 154 (2007) C431, https://doi.org/10.1149/1.2745647.
[51] D. Brugge, A. Datesman, Nuclear waste. Dirty secrets of nuclear power in an era of climate change, Springer Nature Switzerland, Cham, 2024, pp. 21–29, https://doi.org/10.1007/978-3-031-59595-0_3.
[52] C.S. Tully, W.J. Binns, D. Zagidulin, J.J. Noël, Investigating the effect of bentonite compaction density and environmental conditions on the corrosion of copper materials, Mater. Corros. 74 (2023) 1677–1689, https://doi.org/10.1002/maco.202313768.